

REPORT DOCUMENTATION PAGE

Form Approved
OMB No. 0704-0188

1a. REPORT SECURITY CLASSIFICATION UNCLASSIFIED		1b. RESTRICTIVE MARKINGS	
AD-A201 915		3. DISTRIBUTION / AVAILABILITY OF REPORT Approved for public release; distribution unlimited	
		5. MONITORING ORGANIZATION REPORT NUMBER(S)	
6a. NAME OF PERFORMING ORGANIZATION Research Laboratory of Electronics Massachusetts Institute of Technology		6b. OFFICE SYMBOL (if applicable)	
7a. NAME OF MONITORING ORGANIZATION		7b. ADDRESS (City, State, and ZIP Code)	
6c. ADDRESS (City, State, and ZIP Code) 77 Massachusetts Avenue Cambridge, MA 02139		7c. ADDRESS (City, State, and ZIP Code)	
8a. NAME OF FUNDING / SPONSORING ORGANIZATION Office of Naval Research Arctic, Atmospheric and Ionospheric Sci. Div.		8b. OFFICE SYMBOL (if applicable)	
9. PROCUREMENT INSTRUMENT IDENTIFICATION NUMBER N00014-83-K-0258		10. SOURCE OF FUNDING NUMBERS	
8c. ADDRESS (City, State, and ZIP Code) 800 North Quincy Street Arlington, VA 22217		PROGRAM ELEMENT NO.	PROJECT NO. 644-008
		TASK NO.	WORK UNIT ACCESSION NO.
11. TITLE (Include Security Classification) Active and Passive Remote Sensing of Ice			
12. PERSONAL AUTHOR(S) J.A. Kong			
13a. TYPE OF REPORT Semi Annual Report		13b. TIME COVERED FROM 2/1/88 TO 7/31/88	
		14. DATE OF REPORT (Year, Month, Day) November 1, 1988	
		15. PAGE COUNT 52 pp.	
16. SUPPLEMENTARY NOTATION			
17. COSATI CODES		18. SUBJECT TERMS (Continue on reverse if necessary and identify by block number)	
FIELD	GROUP	SUB-GROUP	
19. ABSTRACT (Continue on reverse if necessary and identify by block number) Work by J.A. Kong and his collaborators is summarized here.			
20. DISTRIBUTION / AVAILABILITY OF ABSTRACT <input checked="" type="checkbox"/> UNCLASSIFIED/UNLIMITED <input type="checkbox"/> SAME AS RPT. <input type="checkbox"/> DTIC USERS		21. ABSTRACT SECURITY CLASSIFICATION UNCLASSIFIED	
22a. NAME OF RESPONSIBLE INDIVIDUAL Barbara Passero RLE Contract Reports		22b. TELEPHONE (Include Area Code) (617) 253-2566	
		22c. OFFICE SYMBOL	

DTIC ELECTE
NOV 22 1988
S E

DISTRIBUTION LIST

	<u>DODAAD Code</u>	
Leader, Artic, Atmospheric and Ionospheric Sciences Division Office of Naval Research 800 North Quincy Street Arlington, Virginia 22217	N00014	(1)
Administrative Contracting Officer ONRRR - E19-628 Massachusetts Institute of Technology Cambridge, Massachusetts 02139	N66017	(1)
Director Naval Research Laboratory Attn: Code 2627 Washington, D. C. 20375	N00173	(6)
Defense Technical Information Center Bldg. 5, Cameron Station Alexandria, Virginia 22314	S47031	(12)

Accession For		
NTIS	GRA&I	<input checked="" type="checkbox"/>
DTIC TAB		<input type="checkbox"/>
Unannounced		<input type="checkbox"/>
Justification		
By _____		
Distribution/		
Availability Codes		
Dist	Avail and/or Special	
A-1		



88 1122 011

ACTIVE AND PASSIVE REMOTE SENSING OF ICE

Department of the Navy
Office of Naval Research
Contract N00014-83-K-0258
OSP 93501

SEMI-ANNUAL REPORT

covering the period

February 1, 1988 - July 31, 1988

prepared by

J. A. Kong

Principal Investigator

Massachusetts Institute of Technology
Research Laboratory of Electronics
Cambridge, Massachusetts 02139

ACTIVE AND PASSIVE REMOTE SENSING OF ICE

Principal Investigator: Jin Au Kong

SEMI-ANNUAL PROGRESS REPORT

Under the sponsorship of the ONR contract N00014-83-K-0258, we have published 3 books, 66 journal and conference papers and 10 student theses.

Fully polarimetric scattering properties of earth terrain media are studied with three-layer random medium model. The top scattering layer is modeled as an isotropic random medium which is characterized by a scalar permittivity. The middle scattering layer is modeled as an anisotropic random medium with a symmetric permittivity tensor whose optic axis can be tilted depending on the preferred alignment of the embedded scatterers. The bottom layer is considered as a homogeneous half-space. Volume scattering effects of both random media are described by three-dimensional correlation functions with variances and correlation lengths corresponding to the strengths of the permittivity fluctuations and the physical sizes of the inhomogeneities, respectively. The strong fluctuation theory is used to derive the mean fields in the random media under the bilocal approximation with singularities of the dyadic Green's functions properly taken into consideration. With the discrete scatterer concept, effective permittivities of the random media are calculated by two-phase mixing formulas. Then, the distorted Born approximation is used to calculate the covariance matrix which describes the fully polarimetric scattering properties of the remotely sensed media. The polarimetric information is useful in the identification, classification, and radar image simulation of earth terrain media. *Radon*

To observe polarimetric scattering directly from earth terrain media such as vegetation, meadow, and ice, the three-layer configuration is first reduced to two-layer by removing the top layer. Such media exhibit reciprocity as experimentally manifest in the close proximity of the measured backscattering radar cross sections σ_{VH} and σ_{HV} and theoretically established in the random medium model with a symmetric permittivity tensor. In this case, the covariance matrix is a 3 by 3 matrix with the lower triangle containing elements which are complex conjugates of the corresponding elements in the upper triangle. The results obtained with the two-layer configuration show that polarimetric information carried by the complex correlation coefficient (ρ) is helpful in identifying isotropic versus anisotropic media due to the distinctive characteristics that each of the two media imposes on ρ . For an isotropic medium, the value of ρ is close to 1 over the range of incident angles under the single scattering approximation. Whereas for an anisotropic medium, the magnitude of ρ attains a maximum value at a particular incident angle θ_ρ and decays as the incident angle departs from θ_ρ . Furthermore, the correlation coefficient conveys information about the optic-axis tilted angle of the anisotropic random medium. When the optic axis is not tilted, θ_ρ is at normal incident. As the optic axis becomes tilted, θ_ρ deviates away from normal incident. It should also be noted that the tilt of the optic axis is directly related to the non-zero depolarization terms in the covariance matrix which becomes very small for an untilted anisotropic or isotropic medium. Thus, the fully polarimetric information is important in the remote sensing of earth terrain.

The three-layer random medium has the capability of accounting for polarimetric scattering from earth terrain media under the effects of weather, seasonal variation, and atmospheric conditions such as forest under mist, meadow under fog, and ice under snow. The effects on polarimetric wave scattering due to the top layer are identified by comparing the three-layer model results with those obtained from the two-layer model. Consider first the case of a low-loss scattering layer covering the tilted anisotropic scattering layer. The enhancement of the radar returns due to dry-snow cover on top of first-year sea ice observed in the experimental data can be explained using the three-layer configuration. Also, the low-loss top layer can give rise to the oscillation on the radar returns as a function of incident angle due to the boundary effect. The oscillation can also be seen on the real and imaginary parts of the correlation coefficient (ρ). Interestingly, the magnitude of ρ does not show the oscillation while clearly retaining the similar characteristics as observed directly

from the two-layer configuration. Thus, the correlation coefficient can carry information from both the covering low-loss isotropic layer and the lower tilted anisotropic layer in a rather distinctive manner. As the thickness of the top layer increases, the value of ρ at a given incident angle increases meaning that the top layer can weaken the anisotropic effect of the lower layer. This masking effect is clearly seen when the top layer becomes lossy. In this case, the radar returns are diminished instead of being enhanced. In this application of the random medium model to polarimetric remote sensing of earth terrain, the encountered media are reciprocal and can be characterized by symmetric permittivity tensors.

A radar clutter model is used to simulate fully polarimetric returns for a stepped frequency radar. The purpose is to create synthetic site dependent clutter signatures that can be utilized in a hardware-in-the-loop test system. The fully polarimetric, multi-frequency, multi-incident angle random medium model is employed to generate normalized backscatter coefficients of terrain clutter. This model is used to generate the polarimetric terrain clutter covariance matrices for each of N high resolution range bins, at each of the M discrete frequencies. The random medium model allows us to include the effect of the terrain local incident angle on the clutter covariance matrix elements. In the simulation, we assume that there is a single clutter class within each of the N range bins, although the depression angle may vary from bin to bin. The covariance matrices are decomposed and multiplied by complex Gaussian noise in order to generate the normalized electric fields in the backscattering direction for each of the N range bins, at each of the M discrete frequencies. These fields are then coherently added, taking into account the effects of both terrain elevation and range. This yields a single frequency polarimetric return that a radar would measure from the specified terrain. The radar return for each of the other discrete frequencies is calculated in a similar manner. The result is the clutter's low resolution range polarimetric profile, i.e., the backscattered signal response within the beam footprint of the radar antenna. Each discrete frequency is simulated and the effects of shadowing and overlay are taken into account. The simulation produces coherent phase-history clutter returns which can be coherently superimposed on the target phase-history returns. The combined (or clutter only) returns are processed to obtain either (1) the coherent, high resolution range profile or (2) the noncoherent, autocorrelation range profile.

Supervised and unsupervised classification procedures are developed and applied to synthetic aperture radar (SAR) polarimetric images in order to identify its various earth terrain components. For the supervised classification processing, the Bayes technique is utilized to classify fully polarimetric and normalized polarimetric SAR data. Simpler polarimetric discriminates, such as the unnormalized and normalized magnitude response of the individual receiver channel returns, in addition to the phase difference between the receiver channels are also considered. Covariance matrices are computed for each terrain class from selected portions within the image where ground truth is available, under the assumption that the polarimetric data has a multivariate Gaussian distribution. These matrices are used to train the optimal classifier, which in turn is used to classify the entire image. In this case, classification is based on determining the *distances* between the training classes and the observed feature vector, then assigning the feature vector to belong to that training class for which the distance was minimum. Another processing algorithm based on comparing general properties of the Stokes parameters of the scattered wave to that of simple scattering models is also discussed. This algorithm, which is an unsupervised technique, classifies terrain elements based on the relationship between the orientation angle and handedness, or ellipticity, of the transmitted and received polarization state. These classification procedures will be applied to San Francisco Bay and Traverse City SAR imagery, supplied by the Jet Propulsion Laboratory. It is shown that fully polarimetric classification yields the best overall performance. Also, in some selected areas where the observed amplitudes of the returns are quite different than that of the training data, classification techniques not based on the absolute amplitudes of the returns, e.g., the normalized polarimetric classifier, produced a more consistent result with respect to the ground truth data.

The normalized polarimetric classifier is proposed such that only the relative magnitudes and phases of the polarimetric data will be utilized to discriminate terrain elements. For polarimetric data with arbitrary probability density function (PDF), the distance measures of the normalized polarimetric classifier based on a general class of normalization functions are shown to be equivalent to one another. The normalized polarimetric classifier thus derived will be optimal among all normalization schemes, when the system absolute calibration factors are common to all polarimetric channels. Further assuming a

multivariate complex Gaussian distribution for the un-normalized data, the distance measure of the normalized polarimetric classifier is given explicitly and turns out to be also independent of the number of scatterers. The usefulness of the normalized polarimetric classifier is demonstrated by the classification of trees and grass in the experimental data obtained from Lincoln Laboratory. The classification error is shown to be the smallest among those of magnitude ratio or phase difference classifications.

A three-layer random medium model is developed to study the fully polarimetric scattering properties of earth terrain. The top layer is modeled as an isotropic random medium, the middle layer as an anisotropic random medium, and the bottom layer as a homogeneous half-space. Volume scattering effects of both random media are characterized by correlation functions in which variances and correlation lengths describe strengths of permittivity fluctuations and physical sizes of embedded inhomogeneities, respectively. The anisotropic effect of the middle layer is attributed to specific structure and alignment of the scatterers. With the strong fluctuation theory, the mean fields in the random media are derived under the bilocal approximation with singularities of the dyadic Green's functions properly taken into consideration. With the discrete scatterer concept, effective permittivities of the random media are calculated by two-phase mixing formulas. Then, the distorted Born approximation is used to calculate the covariance matrix which describes the fully polarimetric scattering properties of the terrain and is used in radar image simulation and earth terrain identification and classification.

A two-layer random medium model has been successfully applied to polarimetric remote sensing of earth terrain such as vegetation, meadow, and ice layer. The results obtained with the three-layer configuration have the capability of accounting for polarimetric scattering from earth terrain under the effects of weather, seasonal variation, and atmospheric conditions such as forest under mist, meadow under fog, and ice under snow. The effects on polarimetric wave scattering due to the top layer are identified by comparing the three-layer model results with those obtained from the two-layer model. The enhancement of the radar returns due to dry-snow cover on top of first-year sea ice observed in the experimental data can be explained using the three-layer random medium model. The theoretical results are illustrated by comparing the calculated covariance matrices with the polarimetric measurement data.

There is a considerable interest in determining the optimal polarizations that achieve maximum contrast between two scattering classes in radar polarimetric images for the purpose of terrain discrimination. In this paper, we present a systematic approach for obtaining the optimal polarimetric matched filter which produces maximum contrast between two scattering classes, each represented by its respective covariance matrix.

To accomplish this, we derive a linear weighting vector that maximizes the expected power return ratio, i.e., the contrast ratio between the two scattering classes. The maximization procedure involves solving an eigenvalue problem where the eigenvector yielding this maxima will correspond to the optimal polarimetric matched filter. Then, through use of polarization synthesis, it is demonstrated that when this weighting vector is utilized to process fully polarimetric radar images, the maximum contrast between the two respective classes results. The sub-optimal problem of a fixed transmitting polarization is also considered. In this case, the received polarization is optimized such that a maxima in the contrast ratio is obtained under this constraint. To exhibit the physical significance of this filter, we transform it into its associated transmitting and receiving polarizations, in terms of their horizontal and vertical vector components.

This technique is then applied to radar polarimetry obtained from the Jet Propulsion Laboratory. It is shown, both numerically and through the use of radar imagery, that maximum image contrast can be realized when data is processed with the optimal polarimetric matched filter.

For active and passive microwave remote sensing of sea ice, the two-layer uniaxial random medium model is applied to study the volume scattering and anisotropic effects which are attributed to embedded brine inclusions. In the model, the correlation function is the direct link between the electrical behavior and physical properties of embedded brine inclusions. The spatial distribution, size, elongated structure, and preferred alignment of embedded brine inclusions can be described by variances, correlation lengths, and the form of the correlation function. We have extracted a correlation function of exponential form from the photograph of a horizontal thin section prepared from a sample of artificially grown saline ice that closely resembled Arctic congelation sea ice. It is found that the extracted correlation lengths are consistent with the published average size of brine pockets. With the application of strong fluctuation theory and the bilocal approximation, the

effective permittivity tensor is derived in the low frequency limit for an unbounded uniaxial random medium with two-phase mixtures. Using the extracted correlation length, the effective permittivity tensor is computed as a function of fractional volume of brine inclusions and compared with the in situ dielectric measurements at microwave frequencies of 4.8 and 9.5 GHz. (Electromagnetic theory, sea ice, two-layer uniaxial random medium model, volume scattering, anisotropic, brine inclusions, Arctic congelation sea ice, strong fluctuation theory, bilocal approximation, effective permittivity tensor, two-phase mixture, fractional volume.) 0659 Random media and rough surfaces, 0669 Scattering and diffraction, 0689 Wave propagation

A three-layer random medium model is developed to investigate effects of snow cover on the sea ice signature for microwave remote sensing. The volume scattering and anisotropic effects due to embedded inhomogeneities in the snow-covered sea ice are studied with the wave theory. The snow layer is modelled as an isotropic random medium and the sea ice as an anisotropic random medium. Volume scattering effects are caused by granular ice particles and water contents in snow and by brine inclusions and air bubbles in sea ice, respectively. The anisotropic effect is attributed to the elongated structure of brine inclusions with a preferred alignment between ice platelets. In the random medium model, the essential quantity is the correlation function which contains important physical parameters such as variances and correlation lengths for characterizing the strength of the permittivity fluctuation, the physical size, and the geometrical structure of scatterers. We have extracted correlation function from digitized image of saline ice sample grown in the outdoor tank at CRREL. The calculated correlation lengths are consistent with reported average size of brine pockets.

The strong fluctuation theory is applied to account for the distinct permittivity difference between air, ice particles, water, and brine inclusions. First of all, singularities of the dyadic Green's functions for snow and sea ice are properly considered. Then, the mean fields in both media are derived by the bilocal approximation. With the discrete scatterer concept, effective permittivities for dry snow and first-year sea ice are computed by two-phase mixing formulas. The effective permittivities of sea ice calculated as a function of fractional volume of brine inclusions are found to be consistent with the published results obtained from slab ice samples. For calculating effective permittivities of wet snow and multi-year sea ice, three-phase mixing formulas are used since wet snow consists of air,

ice grains, and water and multi-year sea ice is composed of pure ice, brine inclusions, and air bubbles. Finally, the bistatic scattering and backscattering coefficients are computed with the distorted Born approximation. The results are illustrated by comparing the backscattering coefficients as a function of incident angle with experimental data from controlled field measurements.

A generalized K-distribution is proposed to model the statistics of the fully polarimetric returns from the terrain cover. In the past, K-distribution has been used successfully to characterize the intensity distribution of single polarization returns. Recently, fully polarimetric synthetic aperture radar (SAR) data with polarizations HH, HV, and VV have been proven useful in remote sensing of earth terrain and in this paper we generalize the K-distribution to model fully polarimetric terrain radar clutter. The generalized K-distribution is a better description of the statistics of the SAR polarimetric data than the Gaussian distribution and would be useful in identification and classification of terrain types in the SAR polarimetric data.

In general, all polarization returns of each single polarimetric measurement are correlated with different variances. Therefore, we assume an n-dimensional anisotropic random walk model where the coordinate components of each step are characterized by a covariance matrix and the number of steps or scatterers is of negative binomial distribution with parameter α . The anisotropy in the model refers to the fact that the covariance matrix is not proportional to an identity matrix. A generalized K-distribution for polarimetric data is derived when the average number of steps approaches to infinity. The K-distribution is also generalized to the non-zero mean case, which can be used to model the statistics of transmitted electromagnetic wave through atmosphere. It is found that if a zero-mean K-distributed random vector is normalized by its Euclidean norm, the joint probability distribution of the normalized quantities is independent of the parameter α and is the same as that derived from a zero-mean Gaussian-distributed random vector. The results are illustrated by analyzing the normalized intensity moments of the polarimetric SAR images provided by the Jet Propulsion Laboratory and comparing them with the generalized K-distributed polarimetric model.

The volume scattering effects of snow-covered sea ice are studied with a three-layer random medium model for microwave remote sensing. The strong fluctuation theory and the bilocal approximation are applied to calculate the effective permittivities for snow and sea ice. The wave scattering theory in conjunction with the distorted Born approximation is then used to compute bistatic coefficients and backscattering cross sections. Theoretical results are illustrated by matching experimental data for dry snow-covered thick first-year sea ice at Point Barrow. The radar backscattering cross sections are seen to increase with snow cover for snow-covered sea ice, due to the increased scattering effects in the snow layer. The results derived can also be applied to the passive remote sensing by calculating the emissivity from the bistatic scattering coefficients.

The remote sensing of sea ice is studied with the two-layer random medium model where a correlation function is used to characterize the randomly fluctuating part of the permittivity. Due to the shape and distribution of the brine inclusions, the sea ice is generally anisotropic. We assume the sea ice to be uniaxial and extract correlation functions from a photograph of an artificially grown ice sheet sample. The sizes and distributions of the brine pockets are related to the correlation lengths and the shapes of the correlation functions. The effective permittivity of sea ice is calculated with the strong fluctuation theory assuming a two-phase mixture consisting of pure ice and brine inclusions. The calculated effective permittivities are found to be consistent with the published results obtained from slab ice samples.

A systematic approach for the identification of terrain media is developed using the optimum polarimetric classifier. The covariance matrices for various terrain cover are computed from theoretical models of random medium by evaluating the full polarimetric scattering matrix elements. The optimal classification scheme makes use of a quadratic distance measure and is currently applied to classify a vegetation canopy consisting of both trees and grass. Experimentally measured data are used to validate the classification scheme. Theoretical probability of classification error using the full polarimetric matrix is compared with classification based on single features which include the phase difference between the VV and HH polarization returns. It is shown that the full polarimetric results are optimal and provide better classification performance than single feature measurements. The application of this classification scheme to sea ice will be explored.

The Mueller matrix and polarization covariance matrix are described for polarimetric radar systems. The clutter is modelled by a layer of random permittivity, described by a three-dimensional correlation function, with variance, and horizontal and vertical correlation lengths. This model is applied, using the wave theory with Born approximations carried to the second order, to find the backscattering elements of the polarimetric matrices. It is found that 8 out of 16 elements of the Mueller matrix are identically zero, corresponding to a covariance matrix with four zero elements. Theoretical predictions are matched with experimental data for vegetation fields.

Geophysical media encountered in nature are generally mixtures of dielectrically different materials. When a dielectric mixture is considered macroscopically, i.e., the scale of interest is much larger than the correlation length of the inhomogeneities of the material, it can be assigned an effective permittivity that relates the average macroscopic displacement and the electric field. This effective permittivity can be calculated through a quasistatic analysis which restricts the results of this dielectric mixture theory to cases where the size of the inhomogeneities is much smaller than the wavelength. The limitation resulting from this is that the effective permittivity, which can have complex values, only includes the absorption losses but not the scattering losses.

We have studied the volume scattering effects of snow-covered sea ice with a three-layer random medium model for microwave remote sensing. The strong fluctuation theory and the bilocal approximation are applied to calculate the effective permittivities for snow and sea ice. The wave scattering theory in conjunction with the distorted Born approximation is then used to compute bistatic coefficients and backscattering cross sections. Theoretical results are illustrated by matching experimental data for dry snow-covered thick first-year sea ice at Point Barrow. The radar backscattering cross sections are seen to increase with snow cover for snow-covered sea ice, due to the increased scattering effects in the snow layer. The results derived can also be applied to the passive remote sensing by calculating the emissivity from the bistatic scattering coefficients.

The scattering of electromagnetic waves from a randomly perturbed periodic surface is solved using the Extended Boundary Condition (EBC) method. The scattering from periodic surface is solved exactly using the EBC method and this solution is used in the small perturbation method to solve for the scattered field from a randomly perturbed periodic surface. The random perturbation is modeled as a Gaussian random process and the surface currents and the scattered fields are expanded and solved up to the second order. The theoretical results are illustrated by calculating the bistatic and backscattering coefficients. It is shown that as the correlation length of the random roughness increases, the bistatic scattering pattern of the scattered fields show several beams associated with each Bragg diffraction direction of the periodic surface. When the correlation length becomes smaller, then the shape of the beams become broader. The results obtained using the EBC method is also compared with the results obtained using the Kirchhoff approximation. It is shown that the Kirchhoff approximation results show quite a good agreement with EBC method results for the VV and HH polarized backscattering coefficients for small angles of incidences. However, the Kirchhoff approximation does not give depolarized returns in the backscattering direction whereas the results obtained using the EBC method give significant depolarized returns when the incident direction is not perpendicular to the row direction of the periodic surface.

We have also derived a general mixing formula for discrete scatterers immersed in a host medium. The inclusion particles are assumed to be ellipsoidal. The electric field inside the scatterers is determined by quasistatic analysis, assuming the diameter of the inclusion particles to be much smaller than the wavelength. The results are applicable to general multiphase mixtures, and the scattering ellipsoids of the different phases can have different sizes and arbitrary ellipticity distribution and axis orientation, i.e., the mixture may be isotropic or anisotropic. The resulting mixing formula is nonlinear and implicit for the effective complex dielectric constant, because the approach in calculating the internal field of scatterers is self-consistent. Still, the form is especially suitable for iterative solution. The formula contains a quantity called the apparent permittivity, and with different choices of this quantity, the result leads to the generalized Lorentz - Lorenz formula, the generalized Polder - van Santen formula, and the generalized coherent potential - quasicrystalline approximation formula. Finally, the results are applied to calculating the complex effective permittivity of snow and sea ice.

The study of the strong fluctuation theory for a bounded layer of random discrete scatterers are extended to include high-order co-polarized and cross-polarized second moments. The backscattering cross sections per unit area are calculated by including the mutual coherence of the fields due to the coincidental ray paths and that due to the opposite ray paths which are corresponding to the ladder and cross terms in the Feynman diagrammatic representation. It is proved that the contributions from ladder and cross terms for co-polarized backscattering cross sections are the same, while the contributions for the cross-polarized ones are of the same order. The bistatic scattering coefficients in the second-order approximation for both the ladder and cross terms are also obtained. The enhancement in the backscattering direction can be attributed to the contributions from the cross terms.

We have derived the dyadic Green's function for a two-layer anisotropic medium. The Born approximation is used to calculate the scattered fields. With a specified correlation function for the randomness of the dielectric constant, the backscattering cross sections are evaluated. The analytic expressions for backscattering coefficients are shown to include depolarization effects in the single-scattering approximation. It is also shown that the backscattering cross section (per unit area) of horizontal polarization can be greater than that of vertical polarization even in the case of half-space. The bistatic scattering coefficients are first calculated and then integrated over the upper hemisphere to be subtracted from unity, in order to obtain the emissivity. The principle of reciprocity is then invoked to calculate the brightness temperatures. It is shown that both the absorptive and randomly fluctuating properties of the anisotropic medium affect the behavior of the resulting brightness temperatures both in theory and in actual controlled field measurements. The active and passive results are favorably matched with the experimental data obtained from the first-year and the multiyear sea ice as well as from the corn stalks with detailed ground-truth information.

Electromagnetic wave propagation and scattering in an anisotropic random medium has been examined with Dyson equation for the mean field which is solved by bilocal and nonlinear approximations and with Bethe-Salpeter equation for the correlation of field was derived and solved by ladder approximation. The effective propagation constants are calculated for the four characteristic waves associated with the coherent vector fields propagating in an anisotropic random medium layer, which are the ordinary and extraordinary waves with upward and downward propagating vectors. The z-component of the effective propagation constant of the upward propagating wave is different from the negative of that of the downward propagating wave, not only for the extraordinary wave but also for the ordinary wave. This is due to the tilting of the optic axis which destroys the azimuthal symmetry.

Since both snow and ice exhibit volume scattering effects, we model the snow-covered ice fields by a three-layer random medium model with an isotropic layer to simulate snow, an anisotropic layer to simulate ice, and the bottom one being ground or water. The snow and ice are characterized by different dielectric constants and correlation functions. The theoretical results are illustrated for thick first-year sea ice covered by dry snow at Point Barrow and for artificial thin first-year sea ice covered by wet snow at CRREL. The radar backscattering cross sections are seen to increase with snow cover for snow-covered sea ice, because snow gives more scattering than ice. The results are also used to interpret experimental data obtained from field measurements.

PUBLICATIONS SPONSORED BY THE ONR CONTRACT:

Polarimetric clutter modeling: theory and application (J. A. Kong, F. C. Lin, M. Borgeaud, H. A. Yueh, A. A. Swartz, H. H. Lim, L. M. Novak, and R. T. Shin), *GACIAC PR-88-09*, *The Polarimetric Technology Workshop*, Rocket Auditorium, Redstone Arsenal, U. S. Army Missile Command, Huntsville, Alabama, August 16-19, 1988.

Polarimetric remote sensing of earth terrain with three-layer random medium model (S. V. Nghiem, F. C. Lin, J. A. Kong, R. T. Shin, and H. A. Yueh), *GACIAC PR-88-09*, *The Polarimetric Technology Workshop*, Rocket Auditorium, Redstone Arsenal, U. S. Army Missile Command, Huntsville, AL, Aug. 16-19, 1988.

Radar range profile simulation of terrain clutter using the random medium model (A. A. Swartz, L. M. Novak, R. T. Shin, D. A. McPherson, A. V. Saylor, F. C. Lin, H. A. Yueh, J. A. Kong) to appeared in *GACIAC PR-88-09*, *The Polarimetric Technology Workshop*, Rocket Auditorium, Redstone Arsenal, U. S. Army Missile Command, Huntsville, AL, Aug. 16-19, 1988.

Classification of earth terrain using synthetic aperture radar images (H. Lim, A. A. Swartz, H. A. Yueh, J. A. Kong, R. T. Shin, and J. J. Van Zyl), submitted for publication in *Journal of Geophysical Research*, 1988.

Bayes classification of terrain cover using normalized polarimetric data (H. A. Yueh, A. A. Swartz, J. A. Kong, R. T. Shin, and L. M. Novak), submitted for publication in *Journal of Geophysical Research*, 1988.

Three-layer random medium model for polarimetric remote sensing of earth terrain (H. A. Yueh, S. V. Nghiem, F. C. Lin, J. A. Kong, and R. T. Shin), *IEEE AP-S International Symposium and URSI Radio Science Meeting*, Syracuse, June 6 - 10, 1988.

The optimal polarizations for achieving maximum contrast in radar polarimetry (A. A. Swartz, L. M. Novak, R. T. Shin, H. A. Yueh, and J. A. Kong), *IEEE AP-S International Symposium and URSI Radio Science Meeting*, Syracuse, June 6 - 10, 1988.

Correlation function study for sea ice (F. C. Lin, J. A. Kong, R. T. Shin, A. J. Gow, and S. A. Arcone), *Journal of Geophysical Research*, accepted for publication, 1988.

Effective permittivity of dielectric mixtures (A. Sihvola and J. A. Kong), *IEEE Transactions on Geoscience and Remote Sensing*, Vol.26, no.4, 420-429, July 1988.

The optimal polarizations for achieving maximum contrast in radar polarimetry (A. A. Swartz, H. A. Yueh, J. A. Kong, L. M. Novak, and R. T. Shin), submitted for publication in *Journal of Geophysical Research*, 1988.

Theoretical model for snow-covered sea ice (F. C. Lin, J. A. Kong, R. T. Shin, A. J. Gow, and D. Perovich), *IEEE AP-S International Symposium and URSI Radio Science Meeting*, Syracuse, June 6 - 10, 1988.

K-distribution and polarimetric terrain radar clutter (H. A. Yueh, J. A. Kong, J. K. Jao, and R. T. Shin), *IEEE AP-S International Symposium and URSI Radio Science Meeting*, Syracuse, June 6 - 10, 1988.

Classification of earth terrain using polarimetric synthetic aperture radar imagery (H. H. Lim, A. A. Swartz, H. A. Yueh, J. A. Kong and J. J. van Zyl), *IEEE AP-S International Symposium and URSI Radio Science Meeting*, Syracuse, June 6 - 10, 1988.

Scattering of electromagnetic waves from a periodic surface with random roughness (H. A. Yueh, R. T. Shin, and J. A. Kong), *Journal of Applied Physics*, accepted for publication, 1988.

Self-focusing induced by the ponderomotive effect and the thermal effect (H.C. Han and J. A. Kong), *IEEE AP-S International Symposium and URSI Radio Science Meeting*, Syracuse, June 6 - 10, 1988.

Effect of multiple scattering on the radar cross section of polygonal plate structures (R. G. Atkins and R. T. Shin), *IEEE AP-S International Symposium and URSI Radio Science Meeting*, Syracuse, June 6 - 10, 1988.

Scattering of electromagnetic waves from a periodic surface with random roughness (H. A. Yueh, R. T. Shin, and J. A. Kong), *SPIE Proceedings*, vol. 927, Florida, April 6 - 8, 1988.

Ionospheric modifications by two heater waves (M. C. Lee, K. M. Groves, H. C. Han, J. A. Kong, S. P. Kuo, and H. C. Carlson, Jr.) *the Proceeding of Ionospheric Effect Symposium*, May, 1987.

On the Faraday rotation fluctuations of radio waves (S. V. Nghiem, J. Murad, and M. C. Lee), *the Proceeding of Ionospheric Effect Symposium*, May, 1987.

Scattering of electromagnetic waves from a periodic surface with random roughness (H. A. Yueh, R. T. Shin, and J. A. Kong), *Journal of Applied Physics*, accepted for publication, 1988.

Transient analysis of signal line system in high speed integrated circuits (A. Gu and J. A. Kong), 1987 International Conference on Communication Technology, Nanjing, China, November 3 - 5, 1987.

Exact-image method for Gaussian-beam problems involving a planar interface (I. V. Lindell), *J. Opt. Soc. Am. A*, vol.4, no.12, 2185 - 2190, December 1987.

Identification of Terrain Cover Using the Optimum Polarimetric Classifier (J. A. Kong, A. A. Swartz, H. A. Yueh, L. M. Novak, and R. T. Shin). *Journal of Electromagnetic Waves and Applications*, vol.1, no.4, 1987.

Polarimetric microwave remote sensing of anisotropic earth terrain with strong fluctuation theory (M. Borgeaud, J. A. Kong, and R. T. Shin), *IGARSS 87 and URSI Meeting*, University of Michigan, Ann Arbor, MI, May 18-21, 1987.

Theoretical models for active and passive microwave remote sensing of snow-covered sea ice (F. C. Lin, J. A. Kong, and R. T. Shin), *IGARSS 87 and URSI Meeting*, University of Michigan, Ann Arbor, MI, May 18-21, 1987.

Theoretical models for polarimetric radar clutter (M. Borgeaud, R. T. Shin, and J. A. Kong), *Journal of Electromagnetic Waves and Applications*, vol. 1, no. 1, pp. 73-89, 1987.

Electromagnetic Wave Theory (J. A. Kong), Wiley-Interscience, New York, 696 pages, 1986.

Microwave remote sensing of snow-covered sea ice (M. Borgeaud, J. A. Kong, and F. C. Lin), *1986 International Geoscience and Remote Sensing Symposium*, Zürich, Switzerland, 8-11, September, 1986.

Polarimetric radar clutter modeling with a two-layered anisotropic random medium (M. Borgeaud, J. A. Kong, and R. T. Shin), *International Union of Radio Science Commission F Open Symposium*, University of New Hampshire, Durham, New Hampshire, July 28-August 1, 1986.

Remote sensing of snow-covered sea ice (F. C. Lin and J. A. Kong), *International Union of Radio Science Commission F Open Symposium*, University of New Hampshire, Durham, New Hampshire, July 28-August 1, 1986.

Effective permittivity of dielectric mixtures (A. Sihvola and J. A. Kong), *International Union of Radio Science Commission F Open Symposium*, University of New Hampshire, Durham, New Hampshire, July 28-August 1, 1986.

Modified radiative transfer theory for a two-layer anisotropic random medium (J. K. Lee and J. A. Kong), *National Radio Science Meeting*, Philadelphia, Pennsylvania, June 9-13, 1986.

Theoretical modeling of polarimetric radar clutter (M. Borgeaud, R. T. Shin, and J. A. Kong), *National Radio Science Meeting*, Philadelphia, Pennsylvania, June 9-13, 1986.

Radar cross section prediction using a hybrid method (C. Lee and R. T. Shin), *National Radio Science Meeting*, Philadelphia, Pennsylvania, June 9-13, 1986.

Radar cross section prediction for coated perfect conductors with arbitrary geometries (S. W. Rogers and R. T. Shin), *National Radio Science Meeting*, Philadelphia, Pennsylvania, June 9-13, 1986.

Backscattering and propagation of radar pulses in earth terrain media (F. C. Lin, J. A. Kong, R. T. Shin, and Y. E. Yang), *IEEE IMTC/86 Meeting*, Boulder, Colorado, March 24-27, 1986.

Electromagnetic wave scattering in a two-layer anisotropic random medium (J. K. Lee and J. A. Kong), *J. Optical Society of America*, vol.2, no.12, 2171-2186, December 1985.

Theory of Microwave Remote Sensing (L. Tsang, J. A. Kong, and R. T. Shin), Wiley-Interscience, New York, 613 pages, 1985.

Thermal filamentation instability of millimeter waves in laboratory plasmas (M. C. Lee, J. A. Kong, and S. P. Kuo), *Conference Digest of the 10th International Conference on Infrared and Millimeter Waves*, Florida, December 9-13, 1985.

Saturation of cyclotron maser instability driven by an electron loss-cone distribution (S. P. Kuo and M. C. Lee), *Conference Digest of the 10th International Conference on Infrared and Millimeter Waves*, Florida, December 9-13, 1985.

Analysis of the harmonic gyrotron travelling wave amplifier (S. P. Kuo, S. C. Kuo, B. R. Cheo, and M. C. Lee), *Conference Digest of the 10th International Conference on Infrared and Millimeter Waves*, Florida, December 9-13, 1985.

Passive microwave remote sensing of an anisotropic random medium layer (J. K. Lee and J. A. Kong), *IEEE Trans on Geoscience and Remote Sensing*, vol.GE-23, no.6, 924-932, November 1985.

Active microwave remote sensing of an anisotropic random medium layer (J. K. Lee and J. A. Kong), *IEEE Trans on Geoscience and Remote Sensing*, vol. GE-23, no. 6, 910-923, November 1985

A model for the discrete spectrum of the resonant VLF waves (S. P. Kuo, M. C. Lee, and A. Wolfe), *Proceedings of the workshop on Hydromagnetic Waves in the earth's magnetosphere*, Columbia University, New York, Oct. 17-18, 1985.

Electromagnetic wave scattering by a two-layer anisotropic random medium, (J. K. Lee and J. A. Kong), *IGARSS 85 and URSI Meeting*, University of Massachusetts, Amherst, MA, October 7-9, 1985.

Strong fluctuation theory for scattering, attenuation, and transmission of microwave through snowfall (Y. Q. Jin and J. A. Kong), *IEEE Transactions on Geoscience and Remote Sensing*, vol.GE-23, No.5, 754-760, September 1985.

Electromagnetic characterization of snow and ice for active and passive remote sensing (J. A. Kong), *AGU meeting*, San Francisco, CA, September 1985.

Strong fluctuation theory of random medium and applications in remote sensing (Y. Q. Jin and J. A. Kong), *International Symposium on Antennas and EM Theory (ISAE)*, Beijing, China, August 26-28, 1985.

Mean dyadic Green's function for a two-layer anisotropic random medium: nonlinear approximation to the Dyson equation (J. K. Lee and J. A. Kong), *International Symposium on Antennas and Propagation*, Kyoto, Japan, August 20-22, 1985.

Radar backscattering from snow-covered ice (F. C. Lin, J. K. Lee, J. A. Kong, and R. T. Shin), *Proceedings Snow Symposium V*, Cold Regions Research and Engineering Laboratory, Hanover, New Hampshire, August 13-15, 1985.

Electromagnetic characterization of inhomogeneous media exhibiting volume scattering effects (J. A. Kong), *Workshop on Waves in Inhomogeneous Media*, Schlumberger Doll Research, Ridgefield, Connecticut, August 8-9, 1985.

Polar ionospheric irregularities and possible source mechanisms (M. C. Lee, J. Buchau, H. C. Carlson, Jr., J. A. Klobuchar, and E. J. Weber), *North American Radio Science Meeting and International IEEE/AP-S Symposium*, Vancouver, Canada, June 17-21, 1985.

Generation of E region density irregularities by thermal plasma instabilities (M. C. Lee and S. P. Kuo), *North American Radio Science Meeting and International IEEE/AP-S Symposium*, Vancouver, Canada, June 17-21, 1985.

Ionospheric modifications by HF heaters (M. C. Lee, J. A. Kong, H. C. Carlson, Jr., and S. P. Kuo), *Proceedings of the NATO AGARD Spring 1985 Electromagnetic Wave Propagation Panel Symposium on Propagation effects on military systems in the high latitude region*, Fairbanks, Alaska, June 3-7, 1985.

Ladder and cross terms in second-order distorted Born approximation (Y. Q. Jin and J. A. Kong), *J. Mathematical Physics*, vol.26(5), 994-1011, May 1985.

Wave approach to brightness temperature from a bounded layer of random discrete scatterers (Y. Q. Jin), *Electromagnetics*, vol.4, 323-341, 1984.

Scattering of electromagnetic waves from a randomly perturbed quasiperiodic surface (R. T. Shin and J. A. Kong), *Journal of Applied Physics*, vol.56, 10-21, July 1984.

Microwave thermal emission of periodic surface (J. A. Kong, S. L. Lin, and S. L. Chuang), *IEEE Transactions on Geoscience and Remote Sensing*, vol.GE-22, 377-382, July 1984.

Active and passive microwave remote sensing of layered anisotropic random medium (J. K. Lee and J. A. Kong), *National Radio Science Meeting*, Boston, Massachusetts, June 25-28, 1984.

Modified radiative transfer equation in strong fluctuation approach (Y. Q. Jin and J. A. Kong), *National Radio Science Meeting*, Boston, Massachusetts, June 25-28, 1984.

Scattering of electromagnetic waves by a randomly perturbed quasi-periodic surface (R. T. Shin and J. A. Kong), *National Radio Science Meeting*, Boston, Massachusetts, June 25-28, 1984.

Wave scattering by a bounded layer of random discrete scatterers (Y. Q. Jin and J. A. Kong), *National Radio Science Meeting*, Boulder, Colorado, January 11-13, 1984.

Applied Electromagnetism (L. C. Shen and J. A. Kong), Brooks/Cole, California, 507 pages, 1983.

Dyadic Green's functions for layered anisotropic medium (J. K. Lee and J. A. Kong), *Electromagnetics*, vol.3, 111-130, 1983.

Theory of microwave remote sensing of dense medium (L. Tsang and J. A. Kong), *URSI Symposium*, San Francisco, 1983.

Scattering of electromagnetic waves from a half - space of densely distributed dielectric scatterers (L. Tsang and J. A. Kong), *IEEE/APS Symposium and URSI Meeting*, Houston, Texas, May 23-26, 1983.

Mie scattering of electromagnetic waves by precipitation (Y. Q. Jin and J. A. Kong), *Optical Society of America Topical Meeting on Optical Techniques for Remote Probing of the Atmosphere*, Lake Tahoe, Nevada, January 10-12, 1983.

Thermal microwave emission from a scattering medium with rough surfaces (R. Shin and J. A. Kong), *URSI Symposium*, Boulder, Colorado, January 5-7, 1983.

Remote sensing of soil moisture and vegetation (J. A. Kong, S. L. Lin, S. L. Chuang, and R. T. Shin), *URSI Symposium*, Boulder, Colorado, January 5-7, 1983.

POLARIMETRIC CLUTTER MODELING: THEORY AND APPLICATION

J. A. Kong, F. C. Lin, M. Borgeaud, H. A. Yueh, A. A. Swartz, and H. H. Lim

**Department of Electrical Engineering and Computer Science
and Research Laboratory of Electronics
Massachusetts Institute of Technology
Cambridge, Massachusetts 02139**

R. T. Shin and L. M. Novak

**MIT Lincoln Laboratory
Lexington, MA 02173**

ABSTRACT

The two-layer anisotropic random medium model is used to investigate fully polarimetric scattering properties of earth terrain media. The polarization covariance matrices for the untilted and tilted uniaxial random medium are evaluated using the strong fluctuation theory and distorted Born approximation. In order to account for the azimuthal randomness in the growth direction of leaves in tree and grass fields, an averaging scheme over the azimuthal direction is also applied. It is found that characteristics of terrain clutter can be identified through the analysis of each element of the covariance matrix. Theoretical results are illustrated by the comparison with experimental data provided by MIT Lincoln Laboratory for tree and grass fields.

I. INTRODUCTION

The layered random medium model for terrain cover, in conjunction with the application of electromagnetic wave theory, provides a systematic approach in relating the radar backscatter response to physical properties of geophysical media, where the volume scattering and anisotropic effects are attributed to the embedded inhomogeneities with elongated geometry and preferred alignment. For active and passive microwave remote sensing, the effectiveness of this model has been demonstrated by extraction of physical parameters from data matching for scene interpretation and feature identification [Zuniga *et al.*, 1980; Tsang and Kong, 1981; Tsang *et al.*, 1982; Lee and Kong, 1985; Lin *et al.*, 1988a, b]. In polarimetric microwave remote sensing, the random medium model has also been applied to radar image simulation, terrain clutter identification and classification, and radar range profile simulation of terrain clutter [Shin *et al.*, 1986; Borgeaud *et al.*, 1987a; Borgeaud, 1987b; Kong *et al.*, 1988; Yuch *et al.*, 1988a; Swartz *et al.*, 1988].

The theoretical modeling of earth terrain media is described in Section II. To account for the large permittivity contrast between the background medium and the embedded inhomogeneities, the strong fluctuation theory is applied in Section III, in order to derive the external field which is decomposed into mean (coherent part) and scattered field (incoherent part) components. The mean field is derived using the Feynman diagrammatic technique and bilocal approximation. In Section IV, the effective permittivity tensor of the medium is obtained from the constitutive relation. The effective permittivity tensor is computed in the low frequency limit for an unbounded uniaxial random medium with two-phase mixture. The distorted Born approximation is then used to calculate the scattered field in Section V. The polarization covariance matrices for the untilted and tilted uniaxial random medium, as well as that obtained from the azimuthal averaging of the tilted case are discussed in Section VI. Theoretical calculations of the fully polarimetric random medium model are compared with the experimental data for trees and a grass field supplied by MIT Lincoln Laboratory.

II. TWO-LAYER ANISOTROPIC RANDOM MEDIUM MODEL

The two-layer anisotropic random medium model is applied to simulate earth terrain media such as tree canopy and a grass field. In region 1 of Figure 1, the random medium with height d is characterized by a spatially random permittivity tensor $\bar{\epsilon}_1(\mathcal{F})$. Regions 0 and 2 (air and ground) are considered to be homogeneous media with permittivities ϵ_0 and ϵ_2 , respectively. All three regions are assumed to have the same permeability, μ_0 . The polarimetric radar system is located in region 0. The coordinate system (x, y, z) is

oriented so that the xy plane coincides with the air/clutter interface. Interfaces at $z = 0$ and $z = -d$ are assumed to be planar, extending to infinity on the horizontal plane, and parallel to each other. The volume scattering effect is caused by randomly distributed scatterers embedded in the layer (e.g., moisture content in leaves) while the anisotropic effect is due to the elongated shape and preferred alignment of the scatterers. As shown in Figure 2, the moisture content in trees and grass is modeled as cylindrical scatterers with the preferred alignment in the yz plane. The elongated direction is along the z' -axis and tilted by an angle ψ with respect to the z -axis. Hence, the coordinate system (x', y', z') which describes the orientation of the scatterers is rotated clockwise by an angle ψ about the z -axis. In this manner, the z' -axis can be chosen as the optic axis of the permittivity tensor $\bar{\epsilon}_1(\vec{r})$ [Kong, 1986].

In the polarimetric microwave remote sensing of terrain cover, the polarization covariance matrix is essential for terrain-feature identification and classification [Borgeaud *et al.*, 1987a; Kong *et al.*, 1988]. For a plane wave impinging on the random medium layer, the scattered electric field $\bar{E}_o(\vec{r})$ is related to the incident electric field $\bar{E}_{oi}(\vec{r})$ by

$$\begin{bmatrix} E_{hs} \\ E_{vs} \end{bmatrix} = \frac{e^{i\Delta r}}{r} \begin{bmatrix} f_{hh} & f_{hv} \\ f_{vh} & f_{vv} \end{bmatrix} \begin{bmatrix} E_{hi} \\ E_{vi} \end{bmatrix} \quad (1)$$

where the horizontal and vertical components of the the incident and scattered electric fields are expressed as E_{hi} , E_{hs} , E_{vi} , and E_{vs} , respectively. For reciprocal media, the relation, $f_{vh} = f_{hv}$, is obtained in the backscattering direction. Thus, the covariance matrix is defined as

$$\bar{C} \equiv \lim_{A \rightarrow \infty} \frac{4\pi}{A} \begin{bmatrix} \langle |f_{hh}|^2 \rangle & \langle f_{hh} f_{hv}^* \rangle & \langle f_{hh} f_{vv}^* \rangle \\ \langle f_{hv} f_{hh}^* \rangle & \langle |f_{hv}|^2 \rangle & \langle f_{hv} f_{vv}^* \rangle \\ \langle f_{vv} f_{hh}^* \rangle & \langle f_{vv} f_{hv}^* \rangle & \langle |f_{vv}|^2 \rangle \end{bmatrix} \quad (2)$$

where A is the illuminated area and $\langle X \rangle$ denotes the ensemble average of the random variable X . The covariance matrix is normalized so that the diagonal terms represent the backscattering cross sections per unit area for the HH, HV, and VV polarizations, respectively.

III. STRONG FLUCTUATION THEORY

Consider a linearly polarized time-harmonic electromagnetic plane wave impinging on the random medium. The time-harmonic factor $e^{-i\omega t}$ is used. The propagation vector $\bar{\kappa}_{\alpha}$ at the observation point has the incident angle θ_{α} with respect to the z -axis (Fig. 1) and the azimuthal angle ϕ_{α} . The total electric fields in regions 0 and 1 satisfy the following vector wave equations:

$$\nabla \times \nabla \times \bar{E}_0(\bar{r}) - k_0^2 \bar{E}_0(\bar{r}) = 0 \quad (3)$$

$$\nabla \times \nabla \times \bar{E}_1(\bar{r}) - k_0^2 \frac{\bar{\epsilon}_1(\bar{r})}{\epsilon_0} \cdot \bar{E}_1(\bar{r}) = 0 \quad (4)$$

where $k_0^2 = \omega^2 \mu_0 \epsilon_0$. In the microwave frequency range, the dielectric constants of air and moisture content are very distinct. In order to account for the large permittivity contrast between the host medium and embedded inhomogeneities, a deterministic quantity $\bar{\epsilon}_{g1}$ is introduced in the strong fluctuation theory [Ryzhov and Tamoikin, 1970; Tsang and Kong, 1981; Tsang *et al.*, 1982; Lin *et al.*, 1988a, b]. Equation (4) can then be rewritten as

$$\begin{aligned} \nabla \times \nabla \times \bar{E}_1(\bar{r}) - k_0^2 \frac{\bar{\epsilon}_{g1}}{\epsilon_0} \cdot \bar{E}_1(\bar{r}) &= k_0^2 \left(\frac{\bar{\epsilon}_1(\bar{r}) - \bar{\epsilon}_{g1}}{\epsilon_0} \right) \cdot \bar{E}_1(\bar{r}) \\ &\equiv k_0^2 \bar{Q}_1(\bar{r}) \cdot \bar{E}_1(\bar{r}) \end{aligned} \quad (5)$$

Physically, $\bar{\epsilon}_{g1}$ is the effective permittivity tensor of the medium in the low frequency range where the scattering loss is negligible because the size of scatterers is much smaller than the wavelength of the incident field [Tsang *et al.*, 1985]. Treating the term on the right-hand side of (5) as the effective source, the total electric fields in regions 0 and 1 can be represented in integral forms as follows:

$$\bar{E}_0(\bar{r}) = \bar{E}_0^{(o)}(\bar{r}) + k_0^2 \int_{V_1} d^3\bar{r}_1 \bar{G}_{01}(\bar{r}, \bar{r}_1) \cdot \bar{Q}_1(\bar{r}_1) \cdot \bar{E}_1(\bar{r}_1) \quad (6)$$

$$\bar{E}_1(\bar{r}) = \bar{E}_1^{(o)}(\bar{r}) + k_0^2 \int_{V_1} d^3\bar{r}_1 \bar{G}_{11}(\bar{r}, \bar{r}_1) \cdot \bar{Q}_1(\bar{r}_1) \cdot \bar{E}_1(\bar{r}_1) \quad (7)$$

where the unperturbed electric fields, $\bar{E}_0^{(o)}(\bar{r})$ and $\bar{E}_1^{(o)}(\bar{r})$, are solutions to the homogeneous vector wave equations in (3) and (5) in the absence of the effective source term and the subscript V_1 denotes the volume of region 1. The dyadic Green's functions, $\bar{G}_{01}(\bar{r}, \bar{r}_1)$ and $\bar{G}_{11}(\bar{r}, \bar{r}_1)$, which correspond to the responses at \bar{r} in regions 0 and 1, respectively,

due to a point source at \bar{r}_1 in the anisotropic homogeneous medium with the permittivity tensor $\bar{\epsilon}_{g1}$, are governed by the following vector wave equations:

$$\nabla \times \nabla \times \bar{G}_{01}(\bar{r}, \bar{r}_1) - k_0^2 \bar{G}_{01}(\bar{r}, \bar{r}_1) = 0 \quad (8)$$

$$\nabla \times \nabla \times \bar{G}_{11}(\bar{r}, \bar{r}_1) - k_0^2 \frac{\bar{\epsilon}_{g1}}{\epsilon_0} \cdot \bar{G}_{11}(\bar{r}, \bar{r}_1) = \bar{I} \delta(\bar{r}, \bar{r}_1) \quad (9)$$

When the source and the observation points are in the same region, there is a singularity in the dyadic Green's function, which can be dealt with by separating $\bar{G}_{11}(\bar{r}, \bar{r}_1)$ into principal value $PS\bar{G}_{11}(\bar{r}, \bar{r}_1)$ and singular components, namely,

$$\bar{G}_{11}(\bar{r}, \bar{r}_1) = PS\bar{G}_{11}(\bar{r}, \bar{r}_1) - \frac{\bar{S}_1}{k_0^2} \delta(\bar{r} - \bar{r}_1) \quad (10)$$

Thus, substituting (10) into (7) yields

$$\bar{F}_1(\bar{r}) = \bar{E}_1^{(o)}(\bar{r}) + k_0^2 \int_{V_1} d^3\bar{r}_1 PS\bar{G}_{11}(\bar{r}, \bar{r}_1) \cdot \bar{\xi}_1(\bar{r}_1) \cdot \bar{F}_1(\bar{r}_1) \quad (11)$$

$$\bar{F}_1(\bar{r}) \equiv [\bar{I} + \bar{S}_1 \cdot \bar{Q}_1(\bar{r})] \cdot \bar{E}_1(\bar{r}) \quad (12)$$

$$\bar{\xi}_1(\bar{r}) \equiv \bar{Q}_1(\bar{r}) \cdot [\bar{I} + \bar{S}_1 \cdot \bar{Q}_1(\bar{r})]^{-1} \quad (13)$$

Physically, $\bar{F}_1(\bar{r})$ can be interpreted as the external field [Ryzhov and Tamoikin, 1970].

The external field can be decomposed into a coherent part (mean field) $\langle \bar{F}_1(\bar{r}) \rangle$ and an incoherent part $\bar{F}_1(\bar{r})$ (scattered field) [Tsang *et al.*, 1985]. Under the bilocal approximation, the mean field $\langle \bar{F}_1(\bar{r}) \rangle$ can be expressed as

$$\langle \bar{F}_1(\bar{r}) \rangle = \bar{E}_1^{(o)}(\bar{r}) + k_0^2 \int_{V_r} \int_{V_1} d^3\bar{r}_1 d^3\bar{r}_2 PS\bar{G}_{11}(\bar{r}, \bar{r}_1) \cdot \bar{\xi}_{1,eff}(\bar{r}_1, \bar{r}_2) \cdot \langle \bar{F}_1(\bar{r}_2) \rangle \quad (14)$$

where

$$\bar{\xi}_{1,eff}(\bar{r}_1, \bar{r}_2) = k_0^2 \langle \bar{\xi}_1(\bar{r}_1) \cdot PS\bar{G}_{11}(\bar{r}_1, \bar{r}_2) \cdot \bar{\xi}_1(\bar{r}_2) \rangle \quad (15)$$

Using the index notation, (15) can be expressed as

$$[\bar{\xi}_{1,eff}(\bar{r}_1, \bar{r}_2)]_{lp} = k_0^2 \Gamma_{lmnp} R_\ell(\bar{r}_1, \bar{r}_2) [\bar{G}_{11}(\bar{r}_1, \bar{r}_2)]_{mn} + \Gamma_{lmnp} S_{mn} \delta(\bar{r}_1 - \bar{r}_2) \quad (16)$$

where Equation (10) was used and $\langle \xi_{ilm}(\bar{r}_1) \xi_{inp}(\bar{r}_2) \rangle$ has been replaced with the product of the variance, Γ_{lmnp} ($l, m, n, p = x, y, z$), and the normalized correlation function, $R_\zeta(\bar{r}_1, \bar{r}_2)$. For a statistically homogeneous medium, the normalized correlation function is a function of the displacement between \bar{r}_1 and \bar{r}_2 , i.e.,

$$R_\zeta(\bar{r}_1, \bar{r}_2) = R_\zeta(\bar{r}_1 - \bar{r}_2) \quad (17)$$

Notice that the intrinsic properties of the embedded inhomogeneities are directly related to the volume scattering mechanism through the normalized correlation function in (14).

IV. EFFECTIVE PERMITTIVITY

The effective permittivity tensor for the uniaxial random medium is derived in this section, following the usual approach where the effect of boundary layers is neglected [Tsang and Kong, 1981; Stogryn, 1984]. In an unbounded uniaxial medium, with a quasi-static effective permittivity tensor of the form

$$\bar{\epsilon}_{g1} = \begin{bmatrix} \epsilon_g & 0 & 0 \\ 0 & \epsilon_g & 0 \\ 0 & 0 & \epsilon_{gs} \end{bmatrix} \quad (18)$$

the mean field satisfies the following vector wave equation

$$\nabla \times \nabla \times \langle \bar{F}_1(\bar{r}) \rangle - k_0^2 \frac{\bar{\epsilon}_{g1}}{\epsilon_0} \cdot \langle \bar{F}_1(\bar{r}) \rangle + k_0^2 \int_{-\infty}^{\infty} d^3 \bar{r}_1 \bar{\xi}_{1,eff}(\bar{r}, \bar{r}_1) \cdot \langle \bar{F}_1(\bar{r}_1) \rangle = 0 \quad (19)$$

The dispersion relation, obtained from (19), allows the effective permittivity tensor for the medium to be defined as

$$\bar{\epsilon}_{1,eff}(\bar{k}) \equiv \bar{\epsilon}_{g1} + \epsilon_0 \bar{\xi}_{1,eff}(\bar{k}) = \begin{bmatrix} \epsilon_1 & 0 & 0 \\ 0 & \epsilon_1 & 0 \\ 0 & 0 & \epsilon_{1s} \end{bmatrix} \quad (20)$$

where $\bar{\xi}_{1,eff}(\bar{k})$ is the Fourier transform of $\bar{\xi}_{1,eff}(\bar{r}_1 - \bar{r}_2)$ as given in (16). In the low frequency limit, $\bar{\xi}_{1,eff}(\bar{k})$ can be approximated by

$$[\bar{\xi}_{1,eff}(0)]_{lp} = k_0^2 \Gamma_{lmnp} \int_{-\infty}^{\infty} d^3 \bar{k} \Phi_\zeta(\bar{k}) [\bar{G}_g(\bar{k})]_{mn} + \Gamma_{lmnp} S_{mn} \quad (21)$$

where $\Phi_\epsilon(\bar{k})$ is the Fourier transform of the normalized correlation function $R_\epsilon(\bar{r})$. The Fourier transform of the dyadic Green's function $\bar{G}_g(\bar{r})$ is given as

$$\bar{G}_g(\bar{k}) = \frac{1}{(k_p^2 + k_s^2 - k_0^2 \epsilon_g) k_p^2} \begin{bmatrix} k_y^2 & -k_x k_y & 0 \\ -k_y k_x & k_x^2 & 0 \\ 0 & 0 & 0 \end{bmatrix} - \frac{1}{k_0^2 \epsilon_{gs} \left[k_s^2 + \frac{\epsilon_g}{\epsilon_{gs}} (k_p^2 - k_0^2 \epsilon_{gs}) \right]} \begin{bmatrix} \frac{k_x^2 (k_p^2 - k_0^2 \epsilon_{gs})}{k_p^2} & \frac{k_x k_y (k_p^2 - k_0^2 \epsilon_{gs})}{k_p^2} & k_x k_s \\ \frac{k_y k_x (k_p^2 - k_0^2 \epsilon_{gs})}{k_p^2} & \frac{k_y^2 (k_p^2 - k_0^2 \epsilon_{gs})}{k_p^2} & k_y k_s \\ k_x k_x & k_x k_y & k_s^2 - k_0^2 \epsilon_g \end{bmatrix} \quad (22)$$

in which $k_p^2 = k_x^2 + k_y^2$. Analytical expressions for $\bar{\xi}_{1,ij}(0)$ and the diagonal tensor \bar{S}_1 are shown in Appendix A. For a two-phase mixture consisting of a background medium and scatterers with permittivities ϵ_b and ϵ_s , respectively, $\bar{\xi}_{g1}$ can be evaluated from the following criterion [Tsang and Kong, 1981]:

$$\langle \bar{\xi}_1(\bar{r}) \rangle = 0 \quad (23)$$

From (13) and (23), we obtain

$$\frac{\epsilon_b - \epsilon_g}{\epsilon_0 + S(\epsilon_b - \epsilon_g)} (1 - f_s) + \frac{\epsilon_s - \epsilon_g}{\epsilon_0 + S(\epsilon_s - \epsilon_g)} f_s = 0 \quad (24)$$

$$\frac{\epsilon_b - \epsilon_{gs}}{\epsilon_0 + S_s(\epsilon_b - \epsilon_{gs})} (1 - f_s) + \frac{\epsilon_s - \epsilon_{gs}}{\epsilon_0 + S_s(\epsilon_s - \epsilon_{gs})} f_s = 0 \quad (25)$$

where f_s is the fractional volume of scatterers. Equations (24) and (25) are the anisotropic version of Polder and van Santen's mixing formula [Polder and van Santen, 1946].

V. DISTORTED BORN APPROXIMATION

In the strong fluctuation theory, the original random medium is replaced with an equivalent random medium which has the permittivity, $\bar{\epsilon}_{g1}$. This can be accomplished

without altering the characteristic of the volume scattering effect because the effective source defined in (5) remains intact, that is,

$$k_0^2 \bar{Q}_1(\bar{r}) \cdot \bar{E}_1(\bar{r}) = k_0^2 \bar{\xi}_1(\bar{r}) \cdot \bar{F}_1(\bar{r}) \quad (26)$$

where (12) and (13) have been used. From (6), the total electric field in region 0 can be rewritten as

$$\begin{aligned} \bar{E}_0(\bar{r}) &= \bar{E}_0^{(o)}(\bar{r}) + k_0^2 \int_{V_1} d^3\bar{r}_1 \bar{G}_{01}(\bar{r}, \bar{r}_1) \cdot \bar{\xi}_1(\bar{r}_1) \cdot \bar{F}_1(\bar{r}_1) \\ &\equiv \bar{E}_0^{(o)}(\bar{r}) + \bar{E}_0^s(\bar{r}) \end{aligned} \quad (27)$$

where $\bar{E}_0^s(\bar{r})$ is the scattered electric field due to the effective source. By adopting the concept of the distorted Born approximation in quantum mechanics [Newton, 1966; Schiff, 1968], the scatterers are assumed to be embedded in the equivalent medium with the effective permittivity, $\bar{\epsilon}_{1eff}(0)$ [Lang, 1981], so that the mean field, $\langle \bar{F}_1(\bar{r}) \rangle$, is used to approximate the external field, $\bar{F}_1(\bar{r})$, and the mean dyadic Green's function, $\langle \bar{G}_{01}(\bar{r}, \bar{r}_1) \rangle$, is used to replace $\bar{G}_{01}(\bar{r}, \bar{r}_1)$. The following vector wave equations:

$$\nabla \times \nabla \times \langle \bar{F}_1(\bar{r}) \rangle - k_0^2 \frac{\bar{\epsilon}_{1eff}(0)}{\epsilon_0} \cdot \langle \bar{F}_1(\bar{r}) \rangle = 0 \quad (28)$$

$$\nabla \times \nabla \times \langle \bar{G}_{10}(\bar{r}, \bar{r}_1) \rangle - k_0^2 \frac{\bar{\epsilon}_{1eff}(0)}{\epsilon_0} \cdot \langle \bar{G}_{10}(\bar{r}, \bar{r}_1) \rangle = 0 \quad (29)$$

in conjunction with the symmetric property of the dyadic Green's functions, namely, $\langle \bar{G}_{01}(\bar{r}, \bar{r}_1) \rangle = \langle \bar{G}_{10}(\bar{r}_1, \bar{r}) \rangle^T$, are used to derive the mean field and the mean dyadic Green's function for the scattered electric field which can be written as

$$\bar{E}_0^s(\bar{r}) = k_0^2 \int_{V_1} d^3\bar{r}_1 \langle \bar{G}_{01}(\bar{r}, \bar{r}_1) \rangle \cdot \bar{\xi}_1(\bar{r}_1) \cdot \langle \bar{F}_1(\bar{r}_1) \rangle \quad (30)$$

Physically, the scattered electric field, under the distorted Born approximation, corresponds to the single scattering of the coherent fields [Tsang, *et al.*, 1985]. It is also known as the first-order multiple scattering [Ishimaru, 1978]. After decomposing $\bar{E}_0^s(\bar{r})$ into horizontal and vertical components and making use of (1) and (2), the nine elements of the polarization covariance matrix can be computed.

VI. DATA MATCHING AND APPLICATIONS

Data Matching

For an untilted uniaxial random medium, the optic axis is in the z -direction, $\psi = \psi_i = 0$. For vertically and horizontally polarized incident fields, the single scattering process in the distorted Born approximation does not depolarize the incident field in the backscattering direction and the coefficient f_{hv} vanishes. Hence, the covariance matrix becomes

$$\bar{C} = \sigma \begin{bmatrix} 1 & 0 & \rho\sqrt{\gamma} \\ 0 & 0 & 0 \\ \rho^*\sqrt{\gamma} & 0 & \gamma \end{bmatrix} \quad (31)$$

where σ is the backscattering coefficient for the HH polarization, γ is the copolarization intensity ratio (σ_{vv}/σ_{hh}), and ρ is the normalized correlation coefficient between HH and VV returns given by

$$\rho \equiv \frac{\langle f_{hh} f_{vv}^* \rangle}{\sigma\sqrt{\gamma}} \quad (31b)$$

In general, for the case of tilted uniaxial random medium ($\psi = \psi_i \neq 0$), depolarization effects exist even in the single scattering process, and the nine elements of the covariance matrix are all nonzero, i.e.,

$$\bar{C} = \sigma \begin{bmatrix} 1 & \beta\sqrt{e} & \rho\sqrt{\gamma} \\ \beta^*\sqrt{e} & e & \xi\sqrt{\gamma e} \\ \rho^*\sqrt{\gamma} & \xi^*\sqrt{\gamma e} & \gamma \end{bmatrix} \quad (32)$$

where

$$\beta \equiv \frac{\langle f_{hh} f_{hv}^* \rangle}{\sigma\sqrt{e}} \quad (32a)$$

$$\xi \equiv \frac{\langle f_{hv} f_{vv}^* \rangle}{\sigma\sqrt{e\gamma}} \quad (32b)$$

are the correlation coefficients between the HH and HV and HV and VV channels, respectively. However, when the downward propagation vector $\bar{\kappa}_0$ lies in the yz plane, i.e., $\phi_{0i} = 90^\circ$, both the double refraction phenomenon and the depolarization effect in the

backscattering direction disappear so that $f_{ho} = 0$ [Lee and Kong, 1985a]. Under this condition, the covariance matrix also retains the same form as the untilted case, as shown in (31). It should be noted that the growth directions of leaves in trees and grass fields are not necessarily aligned in one direction. In order to account for the random orientation of the scatterers in the azimuthal direction, an azimuthal averaging scheme [Borgeaud, 1987b] is applied to derive the polarization covariance matrix. It is found that although $f_{ho} \neq 0$, four of the elements in the covariance matrix reduce to zero [Borgeaud *et al.*, 1987a; Kong *et al.*, 1988]. Thus the polarization covariance matrix becomes

$$\bar{C} = \sigma \begin{bmatrix} 1 & 0 & \rho\sqrt{\gamma} \\ 0 & c & 0 \\ \rho^*\sqrt{\gamma} & 0 & \gamma \end{bmatrix} \quad (33)$$

The existence of the four zero elements is due to the fact that the random medium possesses an azimuthal symmetry in a statistical sense. The four zero elements of the covariance matrix indicate that there is no correlation between the copolarization (HH and VV) and cross-polarization (HV) returns, i.e., $\beta = 0$ and $\xi = 0$.

In order to illustrate the random medium model, polarimetric data for forests and grass fields obtained from MIT Lincoln Laboratory are matched with this model. The operating frequency was 35 GHz, and the angle of incidence was 82° . Measured covariance matrices for grass and tree regions, given in Table 1, were calculated from the blocked out regions shown in Figure 7 of [Swartz *et al.*, 1988]. Analysis of this database indicated that there is essentially no correlation between the HH and HV, and between the HV and VV polarimetric returns; from a statistical point of view the terrain clutter exhibited azimuthal symmetry, and therefore $\beta \simeq 0$ and $\xi \simeq 0$. Thus, the form of the covariance matrix shown in (33) was utilized. The corresponding theoretically calculated covariance matrix parameters, also shown in Table 1, were obtained by azimuthal averaging [Borgeaud, 1987b] of the covariance matrices obtained using the two-layer anisotropic random medium model with the application of the strong fluctuation theory and distorted Born approximation.

Applications

The random medium model provides a systematic approach for the design of optimal target detection and classification algorithms [Novak *et al.*, 1987] and the identification of terrain media such as vegetation canopy, forest, and snow-covered fields using the optimum polarimetric classifier [Kong *et al.*, 1988]. The polarization covariance matrices for various

terrain covers were computed from theoretical models of random medium. The optimal classification scheme made use of a quadratic distance measure and was applied to classify a vegetation canopy consisting of both trees and grass; i.e., using the fully polarimetric covariance matrix for the scattered fields, the Bayes likelihood ratio test was performed on specific measurements to classify the terrain into different categories. The Bayes likelihood ratio test has been shown to be optimal in the sense that it minimizes the probability of error [Fukunaga, 1972; Hord, 1986; Richards, 1986; Swain, 1978].

The probabilities of error obtained using fully polarimetric data were compared with the probabilities of error obtained using several single, polarimetrically derived features. For each single feature studied, the corresponding probability density function was derived. Once the probability density functions were known, the Bayes likelihood ratio test was performed to classify terrain elements into different categories. For classification schemes based on single features, closed-form expressions for the probability of error were calculated [Kong *et al.*, 1988].

A supervised Bayes classification was applied to synthetic aperture radar (SAR) polarimetric images in order to identify their various earth terrain components [Lim *et al.*, 1988]. Both fully polarimetric and normalized polarimetric classifications were employed to classify radar imagery. It was again shown, in this case through use of radar images, that fully polarimetric classifications yielded optimal results; however, an optimal normalized classification scheme [Yueh *et al.*, 1988b] indicated improved performance in regions where the absolute backscattering coefficients differed significantly from that of the training regions due to the variation in return power as a function of incident angle.

The Bayes classification is known to give minimum probability of error as long as the statistical distributions of the radar returns are known and the training areas are accurate. However, as noted above, the selected training regions were not sufficient to classify correctly the entire image due to the variation in incident angle over the imaged swath. By employing the random medium model to generate the classifier training data, the effect of the incident angle can be included in the classification scheme.

Another application of the fully polarimetric, multi-incident angle and frequency random medium model is to match training data from various image regions, say at one frequency and during one particular season, and then generate classifier training data which will predict the backscattered response of the terrain at different frequencies and during different seasons of the year. For example, the effects of the winter season can be simulated by adding a layer of snow to a terrain from which training data was recorded

during the summer season. In this manner, data need not be collected for all seasons and at all frequencies. The random medium model can be used to predict the backscattered response based on the initial training data.

APPENDIX A

The normalized correlation function, $R_t(x', y', z')$, for the unbounded uniaxial random medium in the (x', y', z') coordinate frame is assumed to be

$$\exp \left[-\frac{|x'|}{l_p} - \frac{|y'|}{l_p} - \frac{|z'|}{l_s} \right] \quad (A1)$$

so that $\bar{\xi}_{1,ff}$ is given by

$$\bar{\xi}_{1,ff}(0) = \begin{bmatrix} \Gamma_{xxxx}(I+S) & 0 & 0 \\ 0 & \Gamma_{yyyy}(I+S) & 0 \\ 0 & 0 & \Gamma_{zzzz}(I_s+S_s) \end{bmatrix} \quad (A2)$$

where

$$\Gamma_{xxxx} = \Gamma_{yyyy} = \langle \xi^2(\bar{r}) \rangle \equiv \delta_p \quad (A3)$$

$$\Gamma_{zzzz} = \langle \xi_s^2(\bar{r}) \rangle \equiv \delta_s \quad (A4)$$

and

$$\begin{aligned} I = & \frac{\epsilon_0 \zeta}{\pi \epsilon_p (\alpha + 2)} \left\{ \frac{2}{\sqrt{\alpha + 1}} \log \left[\frac{(\sqrt{\alpha - \zeta} + \sqrt{\alpha + 1})(\sqrt{\alpha + 1} + 1)}{\sqrt{\alpha - \zeta} - i\sqrt{\zeta(\alpha + 1)}} \right] \right. \\ & - 2\sqrt{\frac{\alpha - \zeta}{\zeta + 2}} \log \left[\frac{\sqrt{2}(\sqrt{\zeta + 2} - 1)}{\sqrt{\zeta + 2} + i\sqrt{\zeta}} \right] - \frac{\pi}{2} \left. \right\} \\ & - \frac{\epsilon_0}{\pi \epsilon_p (\beta + 2)} \left\{ \frac{2(\beta - \chi)}{\sqrt{\beta + 1}} \log \left[\frac{(\sqrt{\beta - \chi} + \sqrt{\beta + 1})(\sqrt{\beta + 1} + 1)}{\sqrt{\beta - \chi} - i\sqrt{\chi(\beta + 1)}} \right] \right. \\ & \left. + 2\sqrt{(\beta - \chi)(\chi + 2)} \log \left[\frac{\sqrt{2}(\sqrt{\chi + 2} - 1)}{\sqrt{\chi + 2} + i\sqrt{\chi}} \right] + \frac{\pi(\chi + 2)}{2} \right\} \quad (A5) \end{aligned}$$

$$I_s = \frac{2\epsilon_0}{\pi\epsilon_{gs}(\beta+2)} \left\{ \frac{2\beta}{\sqrt{\beta+1}} \log \left[\frac{(\sqrt{\beta-\chi} + \sqrt{\beta+1})(\sqrt{\beta+1} + 1)}{\sqrt{\beta-\chi} - i\sqrt{\chi(\beta+1)}} \right] \right. \\ \left. + 4\sqrt{\frac{\beta-\chi}{\chi+2}} \log \left[\frac{\sqrt{2}(\sqrt{\chi+2}-1)}{\sqrt{\chi+2} + i\sqrt{\chi}} \right] - \frac{\pi\beta}{2} \right\} \quad (A6)$$

where

$$\zeta = \frac{\epsilon_g k_0^2 l_p^2}{\epsilon_0}, \quad \chi = \frac{\epsilon_{gs}}{\epsilon_g} \zeta, \quad \alpha = \zeta + \frac{l_p^2}{l_s^2}, \quad \beta = \frac{\epsilon_{gs}}{\epsilon_g} \alpha \quad (A7)$$

The components of \bar{S}_1 are obtained from the frequency-independent part of (A5) and (A6):

$$S = \frac{\epsilon_0}{\epsilon_g(\eta^2+2)} \left\{ \frac{2\eta^2}{\pi\sqrt{(\eta^2+1)}} \log \left[\frac{\eta\sqrt{\eta^2+1} + \eta^2}{\sqrt{\eta^2+1} - 1} \right] \right. \\ \left. - \frac{\sqrt{2}\eta}{\pi} \log \left[\frac{\sqrt{2}+1}{\sqrt{2}-1} \right] + 1 \right\} \quad (A8)$$

$$S_s = -\frac{\epsilon_0}{\epsilon_{gs}(\eta^2+2)} \left\{ \frac{4\eta^2}{\pi\sqrt{(\eta^2+1)}} \log \left[\frac{\eta\sqrt{\eta^2+1} + \eta^2}{\sqrt{\eta^2+1} - 1} \right] \right. \\ \left. - \frac{2\sqrt{2}\eta}{\pi} \log \left[\frac{\sqrt{2}+1}{\sqrt{2}-1} \right] - \eta^2 \right\} \quad (A9)$$

$$\eta = \sqrt{\frac{\epsilon_{gs} l_p^2}{\epsilon_g l_s^2}} \quad (A10)$$

From (A8) and (A9), it can be shown that S and S_s satisfy the condition [Stogryn, 1983]:

$$2\frac{\epsilon_g}{\epsilon_0} S + \frac{\epsilon_{gs}}{\epsilon_0} S_s = 1 \quad (A11)$$

ACKNOWLEDGEMENTS

This work was supported by ARMY Corp of Engineers contract DACA39-87-K-0022, a SIMTECH contract, NASA Grant NAG5-270, and ONR contract N00014-83-K-0258.

This work was also sponsored by the Defense Advanced Research Projects Agency. The views expressed are those of the authors and do not reflect the official policy or position of the U.S. Government.

REFERENCES

- Borgeaud, M., R. T. Shin, and J. A. Kong (1987a), "Theoretical models for polarimetric radar clutter," *J. of Electromagnetic Waves and Applications*, 1(1), pp. 67-86.
- Borgeaud, M. (1987b), "Theoretical Models for Polarimetric Microwave Remote Sensing of Earth Terrain," Ph. D. Dissertation, Massachusetts Institute of Technology, Jan. 1988.
- Fukunaga, K. (1972), *Introduction to Statistical Pattern Recognition*, Academic Press, New York.
- Ishimaru, A. (1978), *Wave Propagation and Scattering in Random Media*, Vol. 1 and 2, Academic Press, New York.
- Kong, J. A., A. A. Swartz, H. A. Yueh, L. M. Novak, and R. T. Shin (1988), "Identification of terrain cover using the optimum polarimetric classifier," *J. of Electromagnetic Waves and Applications*, 2(2), pp. 171-194.
- Kong, J. A. (1986), *Electromagnetic Wave Theory*, Wiley-Interscience, New York.
- Lang, R. H. (1981), "Electromagnetic backscattering from a sparse distribution of lossy dielectric scatterers," *Radio Science*, 16(1), pp. 15-30.
- Lee, J. K. and J. A. Kong (1985), "Active microwave remote sensing of an anisotropic random medium layer," *IEEE Trans. Geosci. and Remote Sensing*, GE-23(6), pp. 910-923.
- Lim, H. H., A. A. Swartz, H. A. Yueh, J. A. Kong, R. T. Shin, and J. J. van Zyl (1988), "Classification of earth terrain using polarimetric synthetic aperture radar imagery," URSI Meeting, Syracuse, NY, June 6 - 10.

- Lin, F. C., J. A. Kong, R. T. Shin, A. J. Gow, and S. A. Arcone (1988a), "Correlation function study for sea ice," *J. Geophys. Res.*, accepted for publication.
- Lin, F. C., J. A. Kong, R. T. Shin, A. J. Gow, and D. Perovich (1988b), "Theoretical model for snow-covered sea ice," *IEEE AP-S International Symposium & URSI Radio Science Meeting*, Syracuse University, Syracuse, New York, June 6-10.
- Newton, R. G. (1966), *Scattering Theory of Waves and Particles*, McGraw-Hill Book Company, Inc., New York.
- Novak, L. M., M. B. Sechtin, and M. J. Cardullo (1987), "Studies of target detection algorithms that use polarimetric radar data," *IEEE Proceedings of the Nineteenth Asilomar Conference on Circuits, Systems, and Computers*, Pacific Grove, CA, Nov 1-3.
- Papoulis, A. (1984), *Probability, Random Variables, and Stochastic Processes*, McGraw-Hill Book Company, New York.
- Polder, D. and J. H. van Santen (1946), "The effective permeability of mixtures of solids," *Physica*, 12(5), pp. 257-271.
- Richards, J. A. (1986), *Remote Sensing Digital Image Analysis*, Springer-Verlag, New York.
- Ryzhov, Y. A. and V. V. Tamoikin (1970), "Radiation and propagation of electromagnetic waves in randomly inhomogeneous media," *Radiophysics Quantum Electron.*, 13(3), pp. 273-300.
- Schiff, L. I. (1968), *Quantum Mechanics*, 3rd Ed., McGraw-Hill Book Company, Inc., New York.
- Shin, R. T., L. M. Novak, and M. Borgeaud (1986), "Theoretical models for polarimetric radar clutter," *Tenth DARPA/Tri-Service Millimeter Wave Symposium*, U.S. Army Harry Diamond Laboratories, Adelphi, MD, April 8-10.
- Stogryn, A. (1984), "The bilocal approximation for the effective dielectric constant of an isotropic random medium," *IEEE Trans. Ant. and Propag.*, AP-32(5), pp. 517-520.
- Stogryn, A. (1983), "A note on the singular part of the dyadic Green's function in strong fluctuation theory," *Radio Science*, 18(6), pp. 1283-1286.
- Swain, P. H. and S. M. Davis (ed.) (1978), *Remote Sensing: The Quantitative Approach*, McGraw-Hill, New York.

- Swartz, A. A., L. M. Novak, R. T. Shin, D. A. McPherson, A. V. Saylor, F. C. Lin, H. A. Yueh, and J. A. Kong (1988), "Radar range profile simulation of terrain clutter using the random medium model," in *GACIAC PR-88-03, The Polarimetric Technology Workshop*, Rocket Auditorium, Redstone Arsenal, U. S. Army Missile Command, Huntsville, Alabama, August 16-19.
- Tai, C. T. (1971), *Dyadic Green's Functions in Electromagnetic Theory*, Intex Educational Publishers, Scranton, Pennsylvania.
- Tsang, L., J. A. Kong, and R. T. Shin (1985), *Theory of Microwave Remote Sensing*, Wiley-Interscience, New York.
- Tsang, L., J. A. Kong, and R. W. Newton (1982), "Application of strong fluctuation random medium theory to scattering of electromagnetic waves from a half-space of dielectric mixture," *IEEE Trans. Ant. and Propag.*, AP-30(2), pp. 292-302.
- Tsang, L. and J. A. Kong (1981), "Application of strong fluctuation random medium theory to scattering from vegetation-like half space," *IEEE Trans. Geosci. and Remote Sensing*, GE-19(1), pp. 62-69.
- Yueh, H. A., S. V. Nghiem, Lin, F. C., J. A. Kong, and R. T. Shin (1988a), "Three-layer random medium model for polarimetric remote sensing of earth terrain," *IEEE AP-S International Symposium & URSI Radio Science Meeting*, Syracuse University, Syracuse, New York, June 6-10.
- Yueh, H. A., A. A. Swartz, J. A. Kong, R. T. Shin and L. M. Novak (1988b), "Optimal classification of terrain cover using normalized polarimetric data," *J. Geophys. Res.*, accepted for publication.
- Zuniga, M., J. A. Kong, and L. Tsang (1980), "Depolarization effects on the active remote sensing of random media," *J. Appl. Phys.*, 51(5), pp. 2315-2325.

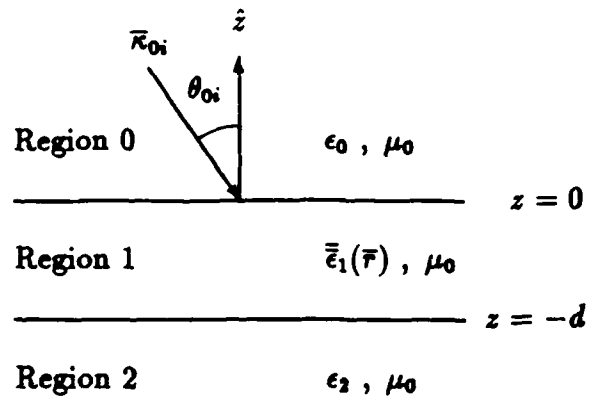


Figure 1 : Anisotropic two-layer random medium configuration.

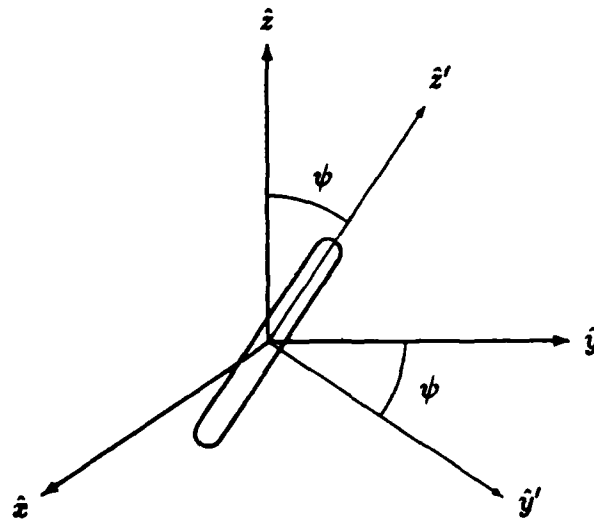
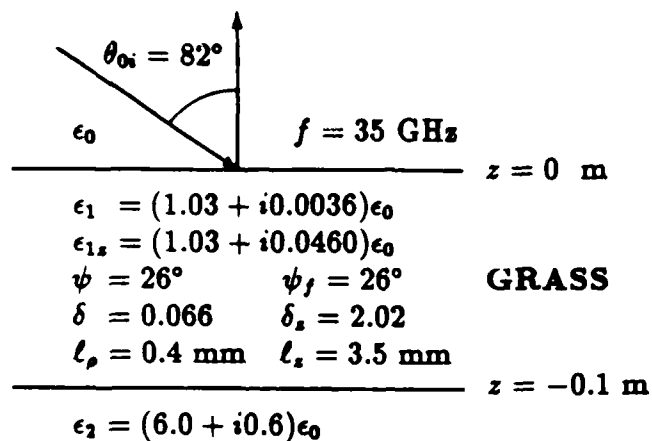


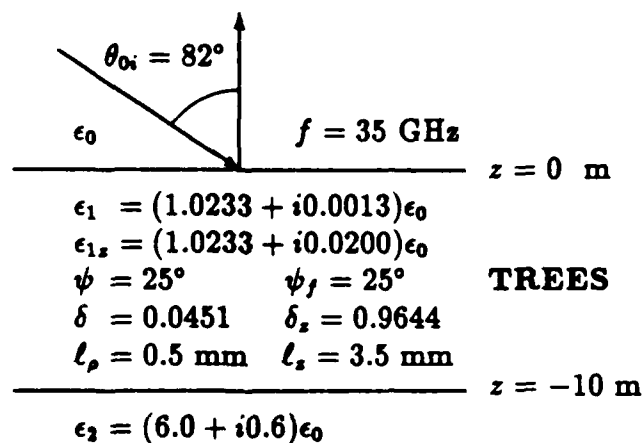
Figure 2 : Geometry of the permittivity tensor in the anisotropic random medium.

(a)



	σ (dB)	e	γ	$ \rho $	ϕ_ρ
Experiment	-14.5	0.19	1.4	0.54	3.5°
Theory	-14.4	0.17	1.3	0.59	3.6°

(b)



	σ (dB)	e	γ	$ \rho $	ϕ_ρ
Experiment	-10.8	0.12	1.2	0.64	0.7°
Theory	-10.6	0.12	1.2	0.65	4.5°

Table 1 : Covariance matrix elements for grass (a) and trees (b).

POLARIMETRIC REMOTE SENSING OF EARTH TERRAIN WITH THREE-LAYER RANDOM MEDIUM MODEL

S. V. Nghiem, F. C. Lin, J. A. Kong, R. T. Shin, H. A. Yueh

Department of Electrical Engineering and Computer Science
and Research Laboratory of Electronics
Massachusetts Institute of Technology
Cambridge, Massachusetts 02139

Abstract

Fully polarimetric scattering of electromagnetic waves from earth terrain media are studied with a three-layer configuration. The inhomogeneous layers are modeled as random media and characterized with three-dimensional correlation functions. The strong fluctuation theory and the distorted Born approximation are used to calculate the covariance matrix which describes the polarimetric radar scattering from the remotely sensed media. Theoretical results are first obtained for two-layer cases and then used to compare with results for three-layer cases to identify the effects on polarimetric wave scattering due to the top layer. A covering dry-snow layer can give rise to the enhancement of radar returns from first-year sea ice and also the oscillation in the real and imaginary parts of the correlation coefficient ρ between the VV and HH returns as a function of incident angle. The magnitude of ρ , however, does not show the oscillation and clearly retains the similar characteristics as observed directly from bare sea ice. When the covering layer is thick or lossy, some polarimetric information from the sea-ice layer is masked out.

I. Introduction

Polarimetric radar scattering from bare terrain fields such as snow, ice, and vegetation has been successfully modeled with the two-layer random medium configuration [1-3]. In this paper, the random medium model is extended to a three-layer configuration to account for fully polarimetric scattering from geophysical media under the effects of weather, diurnal and seasonal variations, and atmospheric conditions such as ice under snow, meadow under fog, and forest under mist. The top scattering layer is modeled as an isotropic random medium which is characterized by a scalar permittivity. The middle scattering layer is modeled as an anisotropic random medium with a symmetric permittivity tensor whose optic axis can be tilted due to the preferred alignment of the embedded scatterers. The bottom layer is considered as a homogeneous half-space. Volume scattering

effects of both random media are described by three-dimensional correlation functions with variances and correlation lengths corresponding to the strengths of the permittivity fluctuations and the physical sizes of the inhomogeneities, respectively. The strong fluctuation theory [4] is used to derive the mean fields in the random media under the bilocal approximation with singularities of the dyadic Green's functions properly taken into account and effective permittivities of the random media are calculated with two-phase mixing formulas. The distorted Born approximation is then applied to obtain the covariance matrix which describes the fully polarimetric scattering properties of the remotely sensed media. The polarimetric information proves to be useful in the identification, classification, and radar image simulation of earth terrain media.

To observe polarimetric scattering directly from terrain media such as snow, ice, and vegetation, the three-layer configuration is first reduced to two-layers by removing the top layer. Such media exhibit reciprocity as experimentally manifested in the close proximity of the measured backscattering radar cross sections $\sigma_{\nu\lambda}$ and $\sigma_{\lambda\nu}$ and theoretically established in the random medium model with symmetric permittivity tensors. The theory is used to investigate the signatures of isotropic and anisotropic random media on the complex correlation coefficient ρ which is helpful in terrain classification [5]. Consideration will also be given to the nonzero depolarization covariance terms which are attributive to the tilt of the optic axis in the anisotropic scattering layer.

The effects on polarimetric wave scattering due to the top layer are identified by comparing the three-layer results with those obtained from the two-layer configuration. The theory is used to explain the enhancement of the radar returns due to a dry-snow cover on top of first-year sea ice, predict the effect of the snow layer on ρ , and study the masking effects on the radar scattering from the ice layer. In this application of the random medium model to polarimetric remote sensing of earth terrain, the encountered media are reciprocal and characterized by symmetric permittivity tensors. In other applications involving a nonreciprocal medium, the permittivity tensor will not be symmetric as in the case of the irregular ionosphere which has been modeled as a gyrotropic random medium [6].

II. Formulation

The scattering configuration is depicted in Figure 1. An electromagnetic wave is incident from air (region 0) to the layered media. Region 1 is a scattering medium with isotropic scatterers randomly embedded such as snow, fog, or mist whose electrical property can be characterized with a spatially dependent permittivity $\epsilon_1(\vec{r})$. Region 2 is an anisotropic random medium containing nonspherical scatterers such as sea ice, grass, or trees which has a spatially dependent permittivity $\epsilon_2(\vec{r})$. Region 3, which can be sea water

or ground, is considered homogenous with a deterministic permittivity ϵ_s . The infinite planar interfaces, the thickness of the layers, and the coordinate system (x, y, z) are shown in Figure 1. Due to the preferred alignment of the nonspherical scatterers, region 2 is effectively uniaxial with the optic axis z' tilted off the z -axis by an angle ψ in the yz -plane as illustrated in Figure 2.

The horizontal and vertical components (E_{hi} and E_{vi} , respectively) of the incident electric field can be related to the horizontal and vertical components (E_{hs} and E_{vs} , respectively) of the scattered electric field by the scattering matrix in the following manner

$$\begin{bmatrix} E_{hs} \\ E_{vs} \end{bmatrix} = \frac{e^{i\theta r}}{r} \begin{bmatrix} f_{hh} & f_{hv} \\ f_{vh} & f_{vv} \end{bmatrix} \begin{bmatrix} E_{hi} \\ E_{vi} \end{bmatrix} \quad (1)$$

In the polarimetric remote sensing of earth terrain, the encountered media are reciprocal. The reciprocity renders $f_{vh} = f_{hv}$. In this case, the fully polarimetric radar backscattering from the layered random medium is characterized by a three by three covariance matrix defined by

$$\bar{C} \equiv \lim_{A \rightarrow \infty} \frac{4\pi}{A} \begin{bmatrix} \langle |f_{hh}|^2 \rangle & \langle f_{hh} f_{vh}^* \rangle & \langle f_{hh} f_{vv}^* \rangle \\ \langle f_{vh} f_{hh}^* \rangle & \langle |f_{vh}|^2 \rangle & \langle f_{vh} f_{vv}^* \rangle \\ \langle f_{vv} f_{hh}^* \rangle & \langle f_{vv} f_{vh}^* \rangle & \langle |f_{vv}|^2 \rangle \end{bmatrix} \quad (2)$$

where A is the illuminated area, the asterisks denote the complex conjugates, and the angular brackets represent the ensemble averages. In terms of the polarimetric radar backscattering coefficients, the covariance matrix (2) can be written as

$$\bar{C} = \begin{bmatrix} \sigma_{hhhh} & \sigma_{hhvh} & \sigma_{hhvv} \\ \sigma_{hhvh}^* & \sigma_{vvhv} & \sigma_{vvhv} \\ \sigma_{hhvv}^* & \sigma_{vvhv}^* & \sigma_{vvvv} \end{bmatrix} \quad (3)$$

Note that the diagonal terms σ_{hhhh} , σ_{vvhv} , and σ_{vvvv} are the conventional radar backscattering coefficients σ_{hh} , σ_{vh} , and σ_{vv} , respectively. Normalized to $\sigma = \sigma_{hh}$, the covariance matrix can be formalized as

$$\bar{C} = \sigma \begin{bmatrix} 1 & \beta\sqrt{e} & \rho\sqrt{\gamma} \\ \beta^*\sqrt{e} & e & \xi\sqrt{\gamma e} \\ \rho^*\sqrt{\gamma} & \xi^*\sqrt{\gamma e} & \gamma \end{bmatrix} \quad (4)$$

where e and γ are the intensity ratios

$$e = \frac{\sigma_{vh}}{\sigma}, \quad \gamma = \frac{\sigma_{vv}}{\sigma} \quad (5)$$

and the correlation coefficients ρ , β , and ξ are

$$\rho = \frac{\sigma_{hhvv}}{\sigma\sqrt{\gamma}}, \quad \beta = \frac{\sigma_{hhvh}}{\sigma\sqrt{e}}, \quad \xi = \frac{\sigma_{vvvv}}{\sigma\sqrt{e\gamma}} \quad (6)$$

From the above definitions, the polarimetric radar backscattering coefficients are determined by the incident and scattered electric fields as follows [7]

$$\sigma_{\mu\tau\nu\kappa} = \lim_{A, r \rightarrow \infty} \frac{4\pi r^2 \langle E_{\mu s}(\vec{r}) E_{\nu i}(\vec{r})^* \rangle}{A E_{\tau i} E_{\kappa s}^*} \quad (7)$$

where μ , ν , τ , or κ can be h or v , and the subscripts i and s denote the incident and scattered fields, respectively. According to (7), the covariance matrix can be calculated when the scattered field is obtained.

III. The Scattered Field

Consider a linearly polarized electromagnetic plane wave incident on the three-layer random medium. For time-harmonic waves, the total fields $\vec{E}_0(\vec{r})$, $\vec{E}_1(\vec{r})$, and $\vec{E}_2(\vec{r})$ in the respective regions 0, 1, and 2 satisfy the following wave equations

$$\nabla \times \nabla \times \vec{E}_0(\vec{r}) - k_0^2 \vec{E}_0(\vec{r}) = 0 \quad (8)$$

$$\nabla \times \nabla \times \vec{E}_1(\vec{r}) - k_0^2 \frac{\epsilon_1(\vec{r})}{\epsilon_0} \vec{E}_1(\vec{r}) = 0 \quad (9)$$

$$\nabla \times \nabla \times \vec{E}_2(\vec{r}) - k_0^2 \frac{\epsilon_2(\vec{r})}{\epsilon_0} \vec{E}_2(\vec{r}) = 0 \quad (10)$$

In the remote sensing of earth terrain, a strong permittivity contrast between the scatterers and the background medium is often encountered. The strong fluctuation theory is therefore necessitated in the calculation of the random-medium effective permittivity. Deterministic permittivities ϵ_{g1} and $\bar{\epsilon}_{g2}$ are respectively introduced in both sides of (9) and (10) and the following vectors

$$k_0^2 \bar{Q}_1(\vec{r}) \cdot \vec{E}_1(\vec{r}) = k_0^2 \left(\frac{\epsilon_1(\vec{r}) - \epsilon_{g1}}{\epsilon_0} \right) \cdot \vec{E}_1(\vec{r}) \quad (11)$$

$$k_0^2 \bar{Q}_2(\vec{r}) \cdot \vec{E}_2(\vec{r}) = k_0^2 \left(\frac{\epsilon_2(\vec{r}) \bar{I} - \bar{\epsilon}_{g2}}{\epsilon_0} \right) \cdot \vec{E}_2(\vec{r}) \quad (12)$$

are treated as the effective sources so that the wave equations (9) and (10) become

$$\nabla \times \nabla \times \bar{E}_1(\bar{r}) - k_0^2 \frac{\epsilon_{g1}}{\epsilon_0} \bar{E}_1(\bar{r}) = k_0^2 \bar{Q}_1(\bar{r}) \cdot \bar{E}_1(\bar{r}) \quad (13)$$

$$\nabla \times \nabla \times \bar{E}_2(\bar{r}) - k_0^2 \frac{\epsilon_2(\bar{r})}{\epsilon_0} \cdot \bar{E}_2(\bar{r}) = k_0^2 \bar{Q}_2(\bar{r}) \cdot \bar{E}_2(\bar{r}) \quad (14)$$

The mean fields in the random media are then derived under the bilocal approximation. In the bilocal approximated Dyson's equations, the possible coincidence of an observation point with a source point gives rise to singularities in the dyadic Green's functions (DGFs). The singularity problem is resolved by decomposing the DGFs into principal value parts with appropriate exclusion volumes and Dirac delta parts with dyadic coefficients \bar{S}_1 and \bar{S}_2 . The quantities ϵ_{g1} , $\bar{\epsilon}_{g2}$, \bar{S}_1 , and \bar{S}_2 are obtained with two-phase mixing formulas and the requirement of secular-term elimination [4]. The variances of the permittivity fluctuations and the effective permittivities $\epsilon_{1,eff}$ and $\bar{\epsilon}_{2,eff}$ for regions 1 and 2 are calculated with the Fourier transform method for a given correlation function [3,4].

With the obtained effective permittivities which account for both the dissipation and the scattering losses, the scattered field under the distorted Born approximation is

$$\begin{aligned} \bar{E}_s(\bar{r}) = & k_0^2 \int_{V_1} d^3\bar{r}_1 \langle \bar{G}_{01}(\bar{r}, \bar{r}_1) \rangle \cdot \bar{\xi}_1(\bar{r}_1) \cdot \langle \bar{F}_1(\bar{r}_1) \rangle \\ & + k_0^2 \int_{V_2} d^3\bar{r}_1 \langle \bar{G}_{02}(\bar{r}, \bar{r}_1) \rangle \cdot \bar{\xi}_2(\bar{r}_1) \cdot \langle \bar{F}_2(\bar{r}_1) \rangle \end{aligned} \quad (15)$$

and the scattered intensity is

$$\begin{aligned} \langle \bar{E}_s(\bar{r}) \cdot \bar{E}_s^*(\bar{r}) \rangle = & \sum_{i,j,h,l,m=1}^2 k_0^4 \int_{V_1} d^3\bar{r}_1 \int_{V_1} d^3\bar{r}_2 C_{\ell 1 j h l m}(\bar{r}_1 - \bar{r}_2) \\ & \cdot \left(\langle \bar{G}_{01ij}(\bar{r}, \bar{r}_1) \rangle \langle \bar{F}_{1h}(\bar{r}_1) \rangle \right) \cdot \left(\langle \bar{G}_{01il}(\bar{r}, \bar{r}_2) \rangle \langle \bar{F}_{1m}(\bar{r}_2) \rangle \right)^* \\ & + \sum_{i,j,h,l,m=1}^2 k_0^4 \int_{V_2} d^3\bar{r}_1 \int_{V_2} d^3\bar{r}_2 C_{\ell 2 j h l m}(\bar{r}_1 - \bar{r}_2) \\ & \cdot \left(\langle \bar{G}_{02ij}(\bar{r}, \bar{r}_1) \rangle \langle \bar{F}_{2h}(\bar{r}_1) \rangle \right) \cdot \left(\langle \bar{G}_{02il}(\bar{r}, \bar{r}_2) \rangle \langle \bar{F}_{2m}(\bar{r}_2) \rangle \right)^* \end{aligned} \quad (16)$$

where V_1 and V_2 are the spaces respectively occupied by regions 1 and 2 and the mean DGFs $\langle \bar{G}_{01}(\bar{r}, \bar{r}_n) \rangle$ and $\langle \bar{G}_{02}(\bar{r}, \bar{r}_n) \rangle$ for $n = 1, 2$ are calculated with the effective permittivities. In (15) and (16), the external fields $\bar{F}_1(\bar{r})$ and $\bar{F}_2(\bar{r})$, the scatterers $\bar{\xi}_1(\bar{r})$ and $\bar{\xi}_2(\bar{r})$, and the correlation functions $C_{\ell 1 j h l m}(\bar{r})$ and $C_{\ell 2 j h l m}(\bar{r})$ are defined as

$$\bar{F}_n(\bar{r}) = [\bar{I} + \bar{S}_n \cdot \bar{Q}_n(\bar{r})] \cdot \bar{E}_n(\bar{r}) \quad , \quad n = 1, 2 \quad (17)$$

$$\bar{\xi}_n(\bar{r}) = \bar{Q}_n(\bar{r}) \cdot [\bar{I} + \bar{S}_n \cdot \bar{Q}_n(\bar{r})]^{-1}, \quad n = 1, 2 \quad (18)$$

$$C_{\xi_{n,jkm}}(\bar{r}_1 - \bar{r}_2) = \langle \xi_{n,jk}(\bar{r}_1) \xi_{n,lm}^*(\bar{r}_2) \rangle, \quad n = 1, 2 \quad (19)$$

In this paper, the following forms of the normalized correlations are used

$$\text{For region 1 : } R_{\xi_1}(\bar{r}) = \exp\left(-\frac{|x| + |y| + |z|}{\ell}\right) \quad (20)$$

$$\text{For region 2 : } R_{\xi_2}(\bar{r}) = \exp\left(-\frac{|x| + |y|}{\ell_p}\right) \exp\left(-\frac{|z|}{\ell_s}\right) \quad (21)$$

The results above are applied in (7) to obtain the covariance matrix of the forms (3) and (4).

IV. Results and Discussions

The three-layer configuration can be reduced to two-layers by removing the top layer to investigate the polarimetric backscattering directly from uncovered earth terrain media. Consider first an electromagnetic wave of 9 GHz incident on an isotropic random medium composed of a background permittivity $\epsilon_{2b} = (3.15 + i0.002)\epsilon_0$ and a 4.5%-volume fraction of isotropic scatterers having a permittivity $\epsilon_2 = (38 + i41)\epsilon_0$ with a correlation length of 1 mm. The strong fluctuation theory gives a variance of 0.32 and an effective permittivity $\epsilon_{2eff} = (3.6 + i0.093)\epsilon_0$. Underlying the random medium of thickness $d_2 = 1.65$ m, the bottom layer has a permittivity $\epsilon_3 = (45 + i40)\epsilon_0$. The physical parameters required to calculate the mean backscattered field are summarized in Figure 3(a). In the case of Figure 3(b), the random medium has the same physical parameters as in the case of Figure 3(a) except that it is effectively anisotropic with correlation lengths $\ell_p = 1$ mm and $\ell_s = 3$ mm for which the strong fluctuation theory yields a variance $\delta_p = 0.22$ and an effective permittivity $\epsilon_{2eff} = (3.52 + i0.08)\epsilon_0$ across the optic axis and $\delta_s = 1.1$ and $\epsilon_{2effs} = (3.99 + i0.458)\epsilon_0$ along the optic axis. For both the isotropic and untilted ($\psi = 0$) anisotropic random media, the depolarization terms $\sigma_{\Lambda\Lambda\Omega\Lambda}$, $\sigma_{\Omega\Lambda\Omega\Omega}$, and $\sigma_{\Omega\Lambda}$ are zero under the first-order distorted Born approximation rendering the covariance matrix of the form

$$\bar{C} = \begin{bmatrix} \sigma_{\Lambda\Lambda} & 0 & \sigma_{\Lambda\Omega\Omega\Omega} \\ 0 & 0 & 0 \\ \sigma_{\Lambda\Omega\Omega\Omega}^* & 0 & \sigma_{\Omega\Omega} \end{bmatrix} \quad \text{or} \quad \bar{C} = \sigma \begin{bmatrix} 1 & 0 & \rho\sqrt{\gamma} \\ 0 & 0 & 0 \\ \rho^*\sqrt{\gamma} & 0 & \gamma \end{bmatrix} \quad (22)$$

In all of the following results, the incident wave vector k_0 is taken to be parallel to the xz -plane though the theory can be used for any arbitrary incident direction. The

conventional backscattering coefficients σ_{AA} and σ_{VV} are plotted as a function of incident angle in Figures 4(a) and 4(b) for the two-layer isotropic and untilted anisotropic cases, respectively. As observed from Figure 4, σ_{VV} crosses over σ_{AA} at an incident angle of about 25° for the anisotropic case whereas, for the isotropic case, σ_{VV} is higher than σ_{AA} over the range of incident angles under consideration. The distinction of the conventional backscattering coefficients σ_{VV} and σ_{AA} associated with the two different random media is, however, not as obvious as that of the polarimetric correlation coefficients ρ as shown in Figure 5 where the isotropic random medium (a) results in ρ with the value of approximately 1.0 over the concerned incident angles and the untilted anisotropic random medium (b) results in ρ with complex values decreased as the incident angle is increased. The correlation coefficient ρ also contains information about the tilt of the optic axis in the anisotropic random medium as illustrated in Figure 6(a) where the maximum magnitude of ρ is at normal incident in the untilted case ($\psi = 0^\circ$) and moves to a larger incident angle as the tilted angle becomes larger. Also shown in Figure 6(b), the phase of ρ does not change sign for $\psi = 0^\circ$ whereas, in the tilted cases, the phase of ρ flips sign at the incident angle where the magnitude of ρ is maximum.

It should be noted that the tilt of the optic axis is also related to the nonzero depolarization terms in the covariance matrix which reduce to zero for an isotropic or untilted anisotropic random medium under the Born approximation as indicated in (22). For the purpose of comparison, shown below are the covariance matrices \bar{C}_i , \bar{C}_a , \bar{C}_{a10} , and \bar{C}_{a20} calculated at an incident angle of 40° respectively for the isotropic, the untilted, the 10° -tilted, and the 20° -tilted anisotropic random media

$$\bar{C}_i = 10^{-3} \begin{bmatrix} 14.2 & 0 & 16.2 - i0.05 \\ 0 & 0 & 0 \\ 16.2 + i0.05 & 0 & 18.3 \end{bmatrix}$$

$$\bar{C}_a = 10^{-3} \begin{bmatrix} 9.95 & 0 & 9.95 - i2.24 \\ 0 & 0 & 0 \\ 9.95 + i2.24 & 0 & 10.7 \end{bmatrix}$$

$$\bar{C}_{a10} = 10^{-3} \begin{bmatrix} 9.37 & 0.64 + i0.97 & 9.62 - i1.48 \\ 0.64 - i0.97 & 0.36 & 0.17 - i1.10 \\ 9.62 + i1.48 & 0.17 + i1.10 & 10.6 \end{bmatrix}$$

$$\bar{C}_{a20} = 10^{-3} \begin{bmatrix} 8.33 & 0.58 + i1.48 & 9.47 + i0.21 \\ 0.58 - i1.48 & 0.96 & 0.79 - i1.68 \\ 9.47 - i0.21 & 0.79 + i1.68 & 10.8 \end{bmatrix}$$

To identify the effects of the covering top layer on the radar backscattering from

the lower layer, the components of covariance matrices are compared for the two-layer and the three-layer configurations. In Figure 7(a), the top layer is a low-loss isotropic random medium of thickness $d_1 = 0.1$ m composed of a background of permittivity $\epsilon_{1b} = \epsilon_0$ and a 25%-volume fraction of isotropic scatterers having a permittivity $\epsilon_{1s} = (3.15 + i0.002)\epsilon_0$ with a correlation length $\ell_s = 0.3$ mm. From the strong fluctuation theory, the variance and the effective permittivity are found to be $\delta = 0.270$ and $\epsilon_{eff} = (1.38 + i4.38 \times 10^{-4})\epsilon_0$, respectively. In Figure 7(b), the top layer is a lossy isotropic random medium with the same physical parameters as in the case of Figure 7(a) except that the imaginary part of the scatterer is now $0.3 \epsilon_0$ which results in $\delta = 0.275$ and $\epsilon_{eff} = (1.38 + i0.039)\epsilon_0$ due to the strong fluctuation theory. In both cases, the bottom layer and the middle anisotropic random medium with a 10° -tilted angle are kept the same as in the case of Figure 3(b). Displayed in Figure 8 are the plots of σ_{hh} and σ_{vv} as a function of incident angle for the two-layer, the low-loss, and the lossy three-layer configurations. In the low-loss case, both σ_{hh} and σ_{vv} are enhanced. Furthermore, the boundary effect is manifested in the form of the oscillation on σ_{hh} and σ_{vv} . The oscillation can also be seen on the real and imaginary parts of the correlation coefficient ρ as shown in Figure 9(a). The magnitude of ρ , however, does not exhibit the oscillation while clearly retaining the same characteristics as observed directly from the two-layer configuration. Thus, the correlation coefficient ρ can carry information from both the covering low-loss isotropic layer and the lower tilted anisotropic layer in a rather distinctive manner. In contrast to the low-loss case, the lossy top layer can diminish both σ_{hh} and σ_{vv} and depress the boundary-effect oscillation as demonstrated in Figure 8. When the thickness of the lossy top layer increases, the behavior of the correlation coefficient ρ becomes more and more similar to the isotropic case (compare Figures 9(b) with 5(a)). In that sense, the lossy top layer can mask out information from the lower anisotropic layer.

As illustrated in this section, the polarimetric information conveyed in the covariance matrix is important in the identification and classification of earth terrain media. Actually, the parameters chosen in the two-layer configuration of Figure 3(b) physically characterize a sea-ice layer over sea water. Due to the physical nature, the random medium model can help remotely identify the ice type with a polarimetric radar. Also in Figure 7(a), the physical parameters correspond to a dry-snow layer covering the sea-ice layer floating on sea water. In this case, it has been shown above that the polarimetric volume scattering effects can reveal useful information from the lower layer even if it is covered under another layer. This is helpful in the remote sensing of the arctic regions in the classification of snow-covered ground and snow-covered sea-ice regions. Since the grain size of the snow cover is modeled with the correlation length [8], the theory can account for diurnal changes which affect the size of snow grains. In the remote sensing of vegetation, the three-layer random medium model is very versatile because it can include the effects of weather and seasonal changes such as meadow under fog or forest under mist. The examples in this section serve the illustration of the physical nature, the usefulness, and

the versatility of the three-layer random medium model in the polarimetric remote sensing of earth terrain.

Acknowledgements

This work was supported by the ARMY Corp of Engineers Contract DACA39-87-K-0022, the SIMTECH Contract, the NASA Grant NAG5-270, and the ONR Contract N00014-83-K-0258.

References

- [1] M. Borgeaud, J. A. Kong, and R. T. Shin, "Polarimetric Radar Clutter Modeling with a Two-Layer Anisotropic Random Medium," *URSI Meeting, Commission F*, University of New Hampshire, Durham, NH, July 28–August 1, 1986.
- [2] M. Borgeaud, R. T. Shin, and J. A. Kong, "Theoretical Models for Polarimetric Radar Clutter," *J. of Electromagnetic Waves and Applications*, 1, 1, p. 67–86, 1987.
- [3] J. A. Kong, F. C. Lin, M. Borgeaud, H. A. Yueh, A. A. Swartz, H. H. Lim, L. M. Novak, and R. T. Shin, "Polarimetric Clutter Modeling: Theory and Application," *GACIAC PR-88-03, The Polarimetric Technology Workshop*, Rocket Auditorium, Redstone Arsenal, U. S. Army Missile Command, Huntsville, Alabama, August 16–19, 1988.
- [4] L. Tsang and J. A. Kong, "Scattering of Electromagnetic Waves From Random Media with Strong Permittivity Fluctuations," *Radio Science*, 16, 3, pp. 303–320, 1981.
- [5] H. H. Lim, A. A. Swartz, H. A. Yueh, J. A. Kong and J. J. van Zyl, "Classification of Earth Terrain Using Polarimetric Synthetic Aperture Radar Imagery," *IEEE AP-S International Symposium and URSI Radio Science Meeting*, Syracuse, June 6 – 10, 1988.
- [6] S. V. Nghiem, "Studies of Correlation Functions in Random Medium Theory," *S.M. Thesis*, M.I.T., May, 1988.
- [7] L. Tsang, J. A. Kong, and R. T. Shin, *Theory of Microwave Remote Sensing*, Wiley-Interscience, New York, 1985.
- [8] F. Vallese and J. A. Kong, "Correlation Studies for Snow and Ice," *J. Appl. Phys.*, 52, 8, p. 4921–4925, August, 1981.

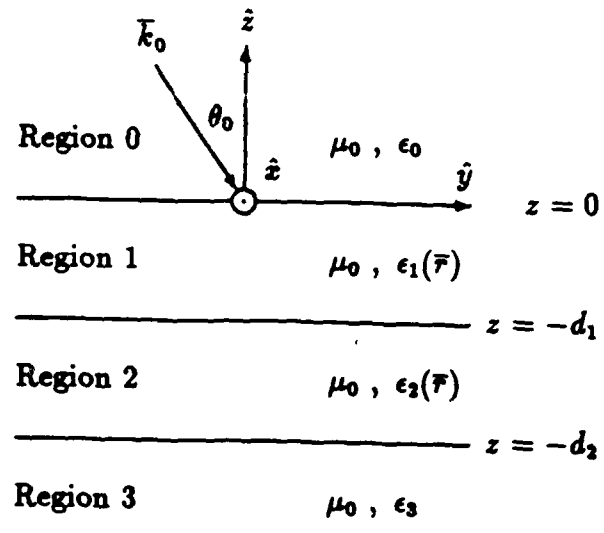


Figure 1 : The three-layer configuration

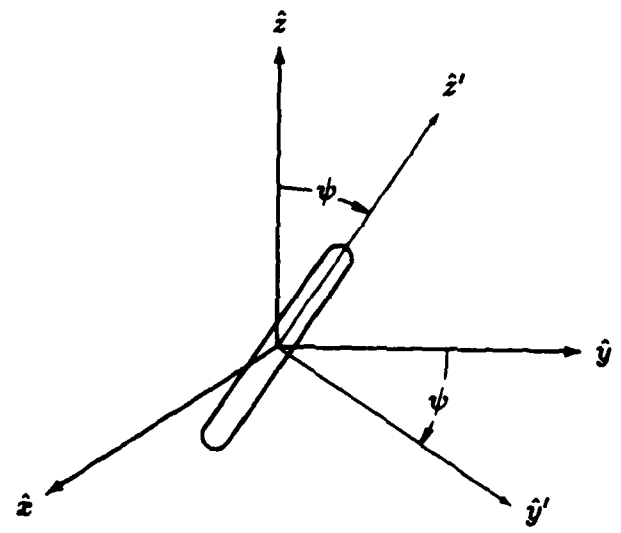


Figure 2 : Geometry of a scatterer in the anisotropic random medium

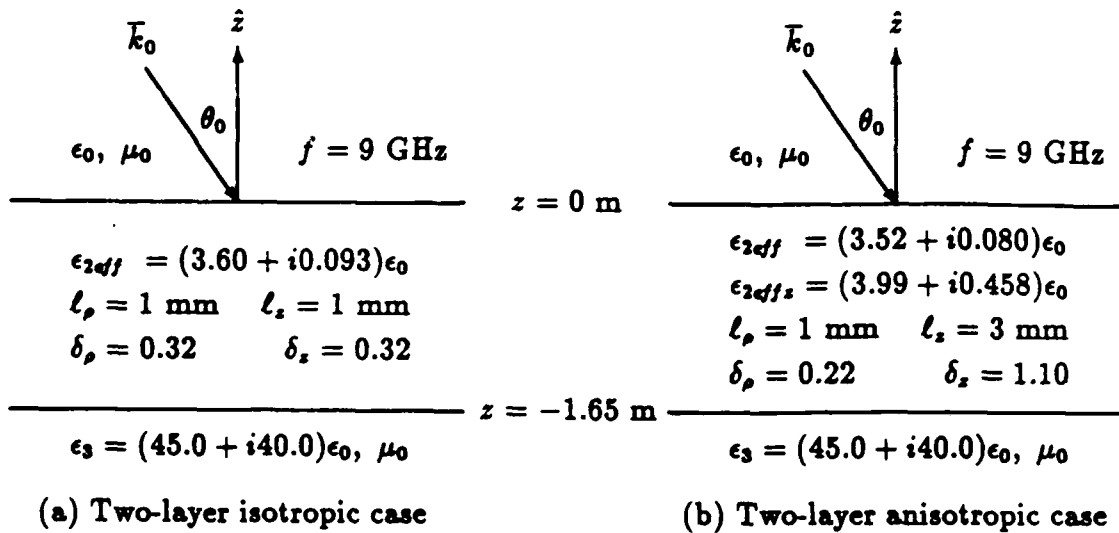


Figure 3 : Physical parameters for the two-layer isotropic and anisotropic media.

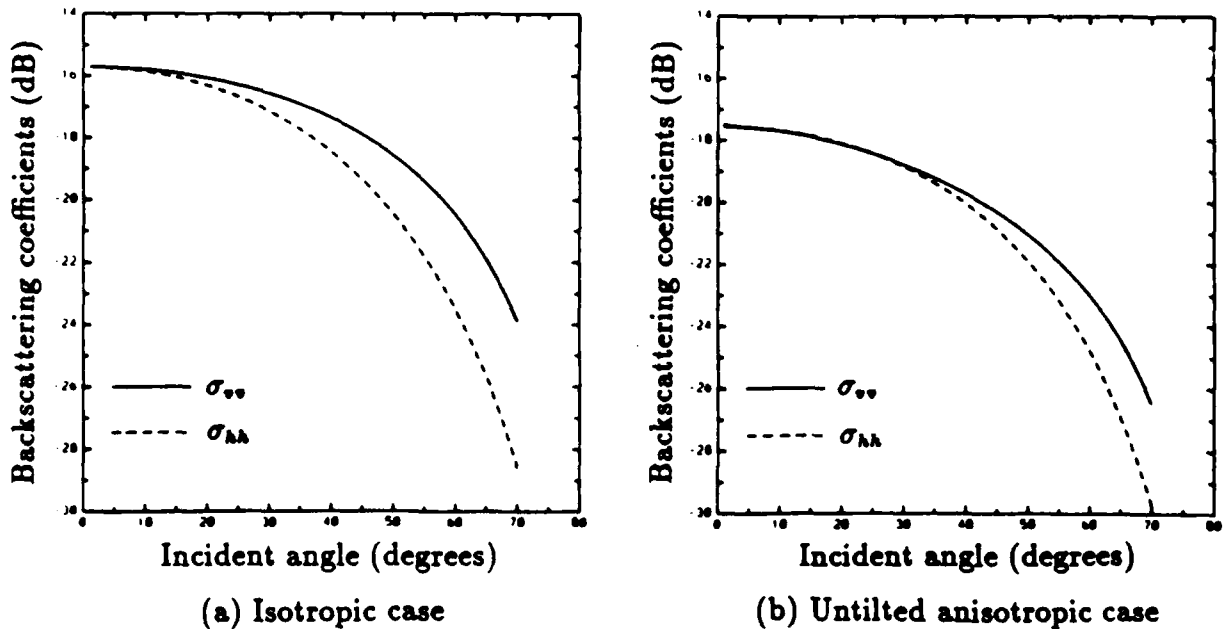
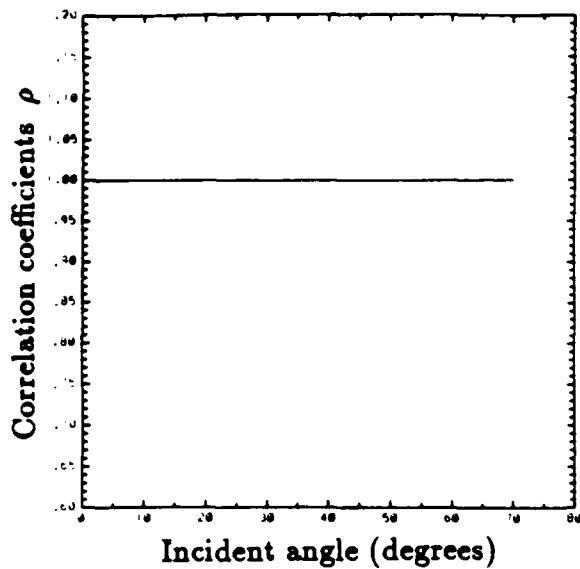
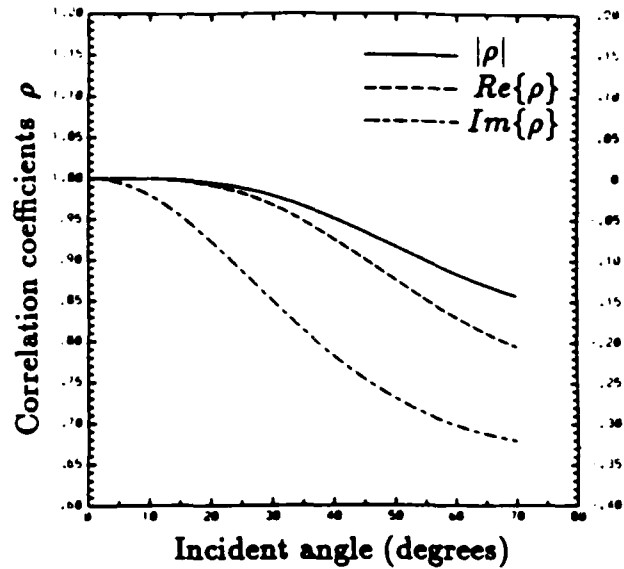


Figure 4 : Comparisons of the conventional backscattering coefficients σ_{hh} and σ_{vv} for the two-layer isotropic and untilted anisotropic cases.

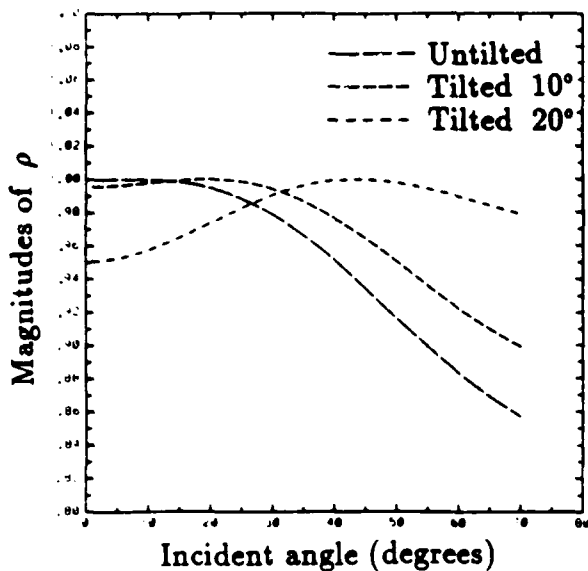


(a) Isotropic case

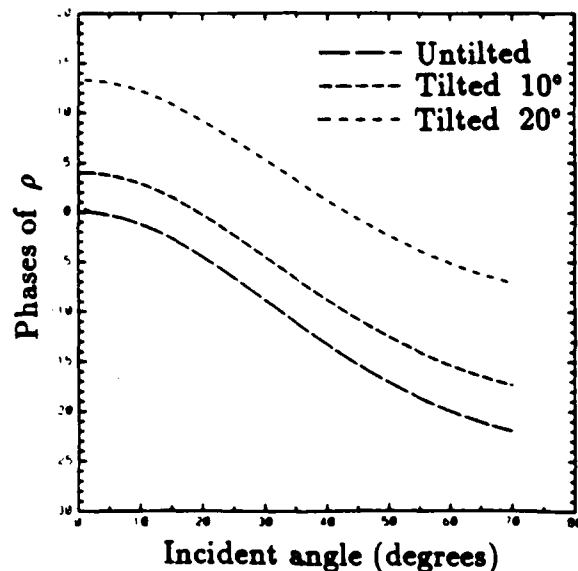


(b) Untilted anisotropic case

Figure 5 : Comparison of the correlation coefficients ρ for the two-layer isotropic and anisotropic cases. In (b), the left vertical scale is for $|\rho|$ and $Re\{\rho\}$ and the right vertical scale is for $Im\{\rho\}$.



(a) Magnitudes of ρ



(b) Phases of ρ

Figure 6 : Magnitudes and phases of ρ for the two-layer anisotropic cases.

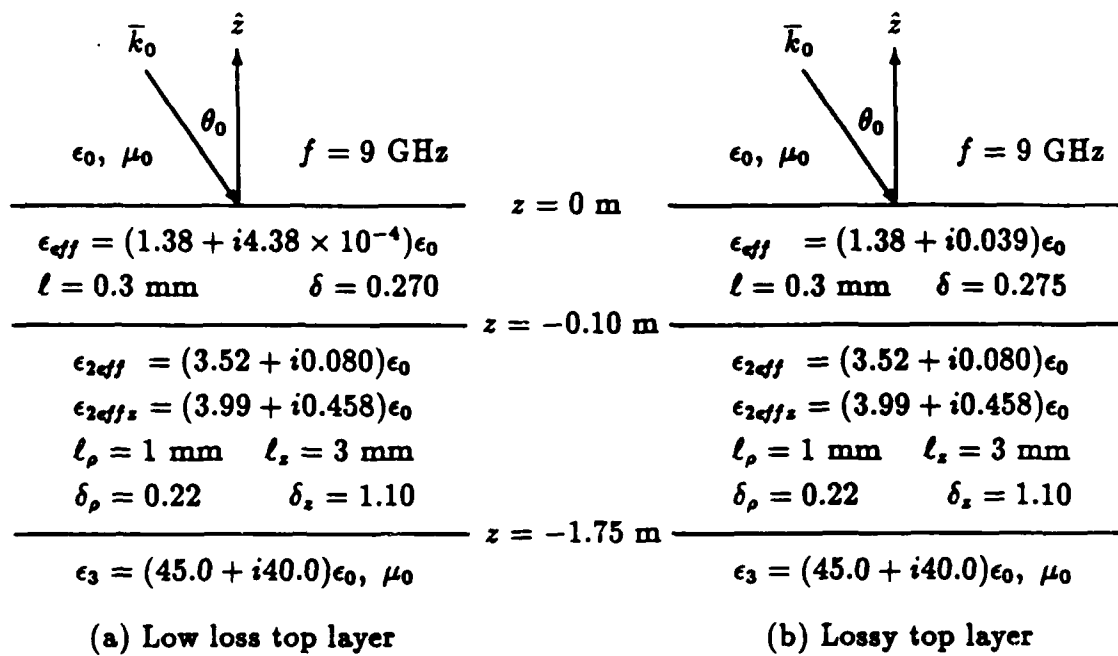
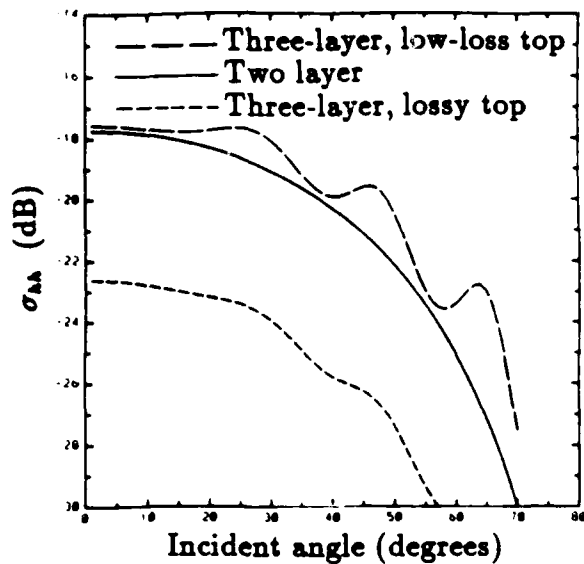
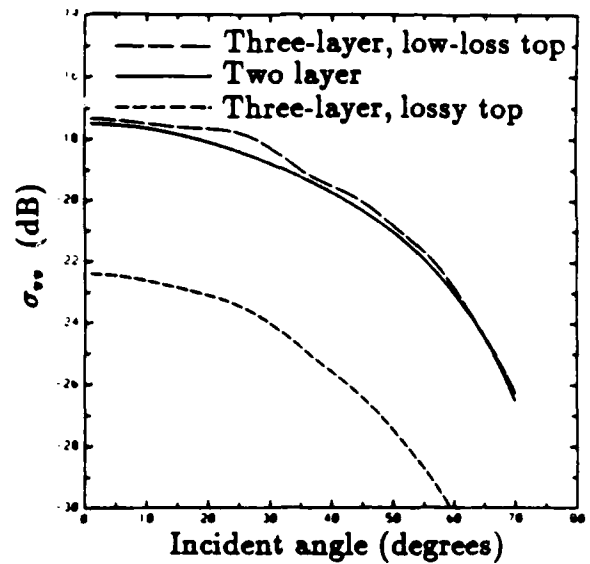


Figure 7 : Physical parameters for the three-layer configurations with low-loss and lossy top layers.

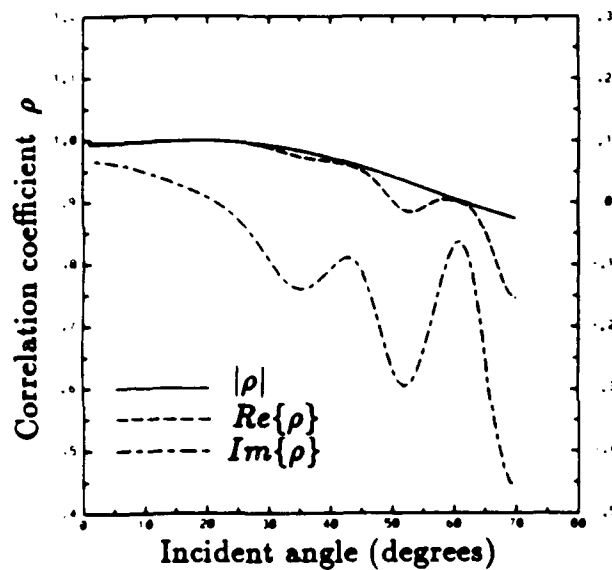


(a) Backscattering coefficient σ_{HH}

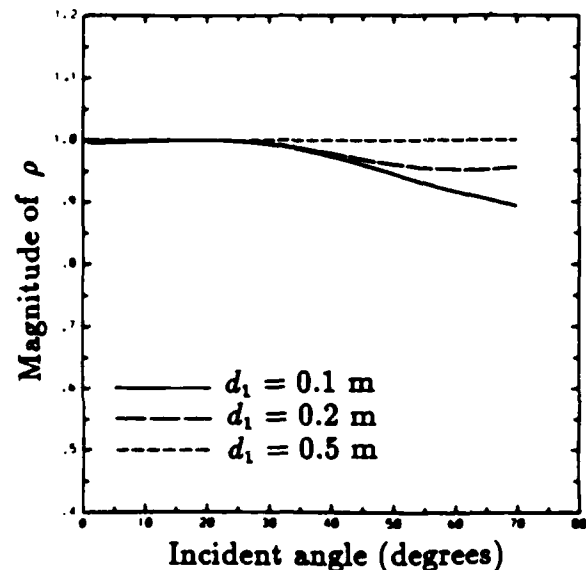


(b) Backscattering coefficient σ_{VV}

Figure 8 : Comparisons of the conventional backscattering coefficients σ_{HH} and σ_{VV} for the three-layer 10° -tilted anisotropic cases with low-loss and lossy top layers.



(a) Three-layer case with low-loss top



(b) Three-layer cases with lossy top

Figure 9 : Correlation coefficients ρ for the three-layer 10° -tilted anisotropic cases with low-loss and lossy top layers. In (a), the left vertical scale is for $|\rho|$ and $Re\{\rho\}$ and the right vertical scale is for $Im\{\rho\}$.